Reciprocity relations

-

May 11, 2006

Using the reciprocity theorem a relation between the seismic reflection response and transmission data can be derived. This relation is used to calculate transmission data from reflection data measured at the surface. In this presentation the steps involved in this calculation are explained in detail and possible pitfalls are discussed. At the end a simple example is given to illustrate the discussed procedure.

1 One-way reciprocity

One-way reciprocity relation of the convolution type:

$$\int_{\partial\mathcal{D}_0}\{P_A^+P_B^- - P_A^-P_B^+\}d^2\mathbf{x}_H = \int_{\partial\mathcal{D}_m}\{P_A^+P_B^- - P_A^-P_B^+\}d^2\mathbf{x}_H \tag{1}$$

One-way reciprocity relation of the correlation type:

$$\int_{\partial\mathcal{D}_0}\{(P_A^+)^*P_B^+ - (P_A^-)^*P_B^-\}d^2\mathbf{x}_H = \int_{\partial\mathcal{D}_m}\{(P_A^+)^*P_B^+ - (P_A^-)^*P_B^-\}d^2\mathbf{x}_H \tag{2}$$

the medium parameters in both states A and B are identical, lossless and 3-D inhomogeneous and the domain $\mathcal{D}$ is source free.

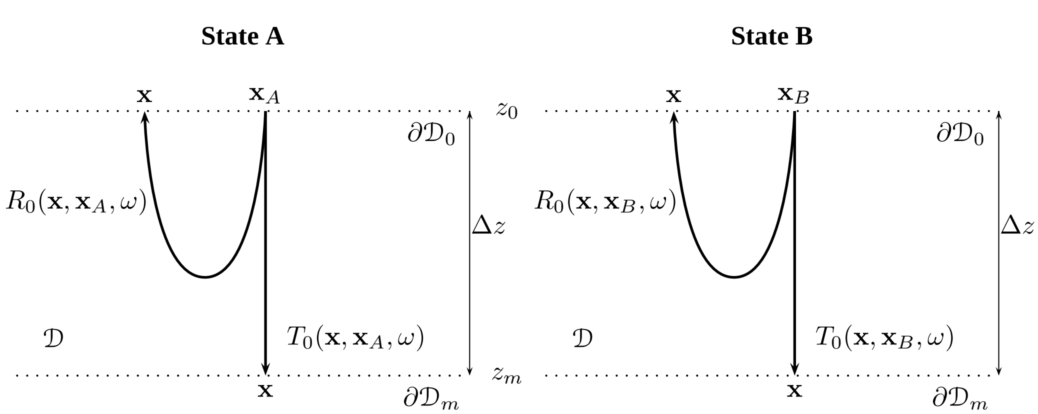

Surface $\partial\mathcal{D}_0$		
Field	**State A**	**State B**
P^+	$\delta(\mathbf{x}_H - \mathbf{x}_{H,A})s_A(\omega)$	$\delta(\mathbf{x}_H - \mathbf{x}_{H,B})s_B(\omega)$
P^-	$R_0(\mathbf{x}, \mathbf{x}_A, \omega)s_A(\omega)$	$R_0(\mathbf{x}, \mathbf{x}_B, \omega)s_B(\omega)$
Surface $\partial\mathcal{D}_m$		
P^+	$T_0(\mathbf{x}, \mathbf{x}_A, \omega)s_A(\omega)$	$T_0(\mathbf{x}, \mathbf{x}_B, \omega)s_B(\omega)$
P^-	0	0

One-way reciprocity relation of the convolution type:

$$s_A s_B \int_{\partial\mathcal{D}_0} \{\delta(\mathbf{x}_H - \mathbf{x}_{H,A})R_0(\mathbf{x}, \mathbf{x}_B) - R_0(\mathbf{x}, \mathbf{x}_A)\delta(\mathbf{x}_H - \mathbf{x}_{H,B})\}d^2\mathbf{x}_H = 0 \tag{3a}$$

$$R_0(\mathbf{x}_A, \mathbf{x}_B) = R_0(\mathbf{x}_B, \mathbf{x}_A) \tag{3b}$$

One-way reciprocity relation of the correlation type:

$$\delta(\mathbf{x}_{H,A} - \mathbf{x}_{H,B}) - \int_{\partial\mathcal{D}_0} R_0^*(\mathbf{x}, \mathbf{x}_A)R_0(\mathbf{x}, \mathbf{x}_B)d^2\mathbf{x}_H = \int_{\partial\mathcal{D}_m} T_0^*(\mathbf{x}, \mathbf{x}_A)T_0(\mathbf{x}, \mathbf{x}_B)d^2\mathbf{x}_H \tag{4}$$

Equation (4) can be used to estimate transmission effects on wave propagation (coda) from reflection data at the surface.

2 From Reflection to Transmission

Dependency on ω is omitted.

$$\delta(\mathbf{x}_{H,A} - \mathbf{x}_{H,B}) - \int_{\partial\mathcal{D}_0} R_0^*(\mathbf{x}, \mathbf{x}_A)R_0(\mathbf{x}, \mathbf{x}_B)d^2\mathbf{x}_H = \int_{\partial\mathcal{D}_m} T_0^*(\mathbf{x}, \mathbf{x}_A)T_0(\mathbf{x}, \mathbf{x}_B)d^2\mathbf{x}_H \tag{5}$$

2.1 Forward model of Transmission response

The transmission response is written as a flux normalized generalized primary propagator W_g in the $\omega - p$ domain:

$$T_0(p, \mathbf{x}_A, z_m, z_0) = W_g(p, \mathbf{x}_A, z_m, z_0) \tag{6}$$

$$T_0(p, \mathbf{x}_A, z_m, z_0) = W_p(p, \mathbf{x}_A, z_m, z_0)C(p, \mathbf{x}_A, \Delta z) \tag{7}$$

with W_p the primary propagator and C the coda operator and $\Delta z = z_m - z_0$. The code operator is a causal function describing the distortion of W_g relative to W_p. The effect of multiple reflections can be delaying, shaping and magnifying the pulse transmitted through a layered sequence.

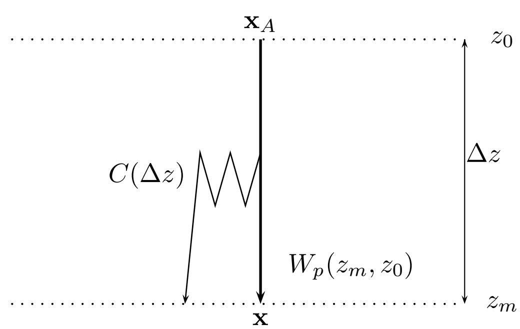

O'Doherty and Anstey [] found that the coda operator $C(\omega)$ is related to the power spectrum of the reflection coefficient. See discussion in proefschrift Frederic: pages 18-19-20 section 2.4. For the current discussion we only need the know that C can be written as:

$$C(p, \mathbf{x}_A, \Delta z) = \exp(-\mathcal{A}(p)\Delta z) \tag{8}$$

$$W_p(p, \mathbf{x}_A, z_m, z_0) = \exp(-j\omega \int_{z_0}^{z_m} (c^{-2}(z) - p^2)^{\frac{1}{2}} dz) \tag{9}$$

$$W_p^*(p, \mathbf{x}_A, z_m, z_0) W_p(p, \mathbf{x}_A, z_m, z_0) \approx 1.0 \tag{10}$$

$$C(p, \mathbf{x}_A, \Delta z) = \exp(-\mathcal{A}(p)\Delta z) \tag{11}$$

$$T^*(p, \mathbf{x}_A, \Delta z) T(p, \mathbf{x}_A, \Delta z) = C^*(p, \mathbf{x}_A, \Delta z) C(p, \mathbf{x}_A, \Delta z) \tag{12}$$

$$C^*(p, \mathbf{x}_A, \Delta z) C(p, \mathbf{x}_A, \Delta z) = \exp(-2\Re\{\mathcal{A}(p)\}\Delta z) \tag{13}$$

$\Re\{\mathcal{A}\}(p)$ is the real part of $\mathcal{A}(p)$. Note that $\mathcal{A}(p)$ is written as a function of the ray-parameter p.

Replace integral with discrete notation in vectors:

$$\int_{\partial \mathcal{D}_0} R_0^*(\mathbf{x}, \mathbf{x}_A) R_0(\mathbf{x}, \mathbf{x}_B) d^2\mathbf{x}_H \equiv \boldsymbol{R}_0^H(\mathbf{x}, \mathbf{x}_A) \boldsymbol{R}_0(\mathbf{x}, \mathbf{x}_B) \tag{14}$$

$$= \left(R_0^*(\mathbf{x}_0, \mathbf{x}_A) \ldots R_0^*(\mathbf{x}_i, \mathbf{x}_A) \ldots R_0^*(\mathbf{x}_N, \mathbf{x}_A) \right) \begin{pmatrix} R_0(\mathbf{x}_0, \mathbf{x}_A) \\ \vdots \\ R_0(\mathbf{x}_i, \mathbf{x}_A) \\ \vdots \\ R_0(\mathbf{x}_N, \mathbf{x}_A) \end{pmatrix}$$

extend vectors to matrices by including more shot records (different $\mathbf{x}_A$) Matrices for propagation and reflection including all effects due to interbed multiples with a fixed spread acquisition geometry:

$$\mathbf{C} = \begin{pmatrix} C(\mathbf{x}_{r,0}, \mathbf{x}_{s,0}) & \dots & C(\mathbf{x}_{r,0}, \mathbf{x}_{s,N}) \\ \vdots & \ddots & \vdots \\ C(\mathbf{x}_{r,M}, \mathbf{x}_{s,0}) & \dots & C(\mathbf{x}_{r,M}, \mathbf{x}_{s,N}) \end{pmatrix} \tag{15a}$$

$$\mathbf{R} = \begin{pmatrix} R(\mathbf{x}_{r,0}, \mathbf{x}_{s,0}) & \dots & R(\mathbf{x}_{r,0}, \mathbf{x}_{s,N}) \\ \vdots & \ddots & \vdots \\ R(\mathbf{x}_{r,M}, \mathbf{x}_{s,0}) & \dots & R(\mathbf{x}_{r,M}, \mathbf{x}_{s,N}) \end{pmatrix} \tag{15b}$$

represents a fixed spread acquisition geometry. Using the matrices the integral equations becomes:

$$\mathbf{T}^H\mathbf{T} = \mathbf{I} - \mathbf{R}^H\mathbf{R} \tag{16}$$

$$\mathbf{T}^H\mathbf{T} = (\mathbf{W_p}\mathbf{C})^H\mathbf{W_p}\mathbf{C} = \mathbf{C}^H\mathbf{C} \tag{17}$$

$$\mathbf{C}^H\mathbf{C} = \mathbf{I} - \mathbf{R}^H\mathbf{R} \tag{18}$$

$\mathbf{C}$ is measured at $\partial\mathcal{D}_m$ and $\mathbf{R}$ is measured at $\partial\mathcal{D}_0$. Superscript H denotes complex-conjugate transpose. For fixed spread geometry both $\mathbf{R}$ and $\mathbf{T}$ matrices are symmetric (not Hermitian) due to the reciprocity relation between source and receiver positions.

We need to resolve $\mathbf{C}$ from $\mathbf{C}^H\mathbf{C}$ and make the assumption that:

$$\mathbf{C} = \mathbf{L}\boldsymbol{\Lambda}_c\mathbf{L}^H \tag{19}$$

$$\boldsymbol{\Lambda}_c(p) = \exp\{-\underset{\sim}{\mathbf{A}}(p)(\omega)\Delta z_{tot}\} \tag{20}$$

$$\boldsymbol{\Lambda}_c(p) = \begin{pmatrix} e^{-\mathcal{A}(p_1)\Delta z_{tot}} & 0 & \dots & 0 \\ 0 & e^{-\mathcal{A}(p_2)\Delta z_{tot}} & \dots & 0 \\ \dots & \dots & \dots & \dots \\ 0 & 0 & \dots & e^{-\mathcal{A}(p_N)\Delta z_{tot}} \end{pmatrix} \tag{21}$$

where $\underset{\sim}{\mathbf{A}}(p)$ is a diagonal matrix. For plane waves in 1D media $\mathbf{C}$ is a circulant matrix which has the property that its Fourier transform is equal to its eigenvalues (see [Sjöström, 1996] for proof): $\boldsymbol{\Lambda}_c = \mathcal{F}_{x\to k_x}\{\mathbf{C}\}$ $\mathbf{C} = \mathbf{F}^H\boldsymbol{\Lambda}_c\mathbf{F}$

Correlation of coda matrix:

$$\mathbf{C}^H\mathbf{C} = \mathbf{L}\boldsymbol{\Lambda}_c^H\boldsymbol{\Lambda}_c\mathbf{L}^H \tag{22}$$

$$\boldsymbol{\Lambda}_c^H\boldsymbol{\Lambda}_c = \exp\{-2\mathcal{R}\{\underset{\sim}{\mathbf{A}}(p)\}\Delta z_{tot}\} \tag{23}$$

$$\boldsymbol{\Lambda}_c^H\boldsymbol{\Lambda}_c = \begin{pmatrix} e^{-2\mathcal{R}\{\mathcal{A}_1\}} & 0 & \dots & 0 \\ 0 & e^{-2\mathcal{R}\{\mathcal{A}_2\}} & \dots & 0 \\ \dots & \dots & \dots & \dots \\ 0 & 0 & \dots & e^{-2\mathcal{R}\{\mathcal{A}_N\}} \end{pmatrix} \tag{24}$$

Using the assumptions about the coda operator the $\underset{\sim}{\mathbf{A}}(p)$ operator can be retrieved from its real part. The main assumption states that the elements $A_l(\omega)$ of $\underset{\sim}{\mathbf{A}}(p)$ are the Fourier transforms of causal filters in the time domain. This is true for 1D media, since in that case $\underset{\sim}{\mathbf{A}}$ is the spatial fourier transform of $\underset{\sim}{\mathbf{C}}$, so $A_l(\omega) = \tilde{\mathcal{A}}_l(k_{x,l}, \omega)$. Note that before the temporal Fourier transforms yields the causal filters, the diagonal elements must to be scaled from wavenumber k_x to propagation angle p with $\frac{1}{\omega}(k_x = p\omega)$. Also in the general 3-D case a scaling of the diagonal of $\underset{\sim}{\mathbf{\Lambda}}_c$ with $\frac{1}{\omega}$ is reguired before the $\tilde{A}_l(\omega)$ can be interpreted as the Fourier transforms of causal filters in the time domain.

Now $\mathcal{R}\{\mathcal{A}_i\}$ can be calculated using:

$$2\mathcal{R}\{\mathcal{A}_i\} = \ln(\Lambda_{c,i}^H \Lambda_{c,i}) \tag{25}$$

Since in general $\Lambda_{c,i}^H \Lambda_{c,i}$ is a complex number a complex logarithm $\ln(a + ib)$ must be taken:

$$\mathcal{R}\{\ln(a + ib)\} = (a^2 + b^2)^{\frac{1}{2}} \tag{26}$$

$$\mathcal{I}\{\ln(a + ib)\} = atan(\frac{b}{a}) \tag{27}$$

Reconstruction of $\mathcal{A}_i(p)$ from its real part is possible because $\mathcal{A}_i(p)$ is a causal function and with the definition of the analytic signal:

$$A(\omega) = \mathcal{R}\{A(\omega)\} + \frac{1}{j\pi}\int_{-\infty}^{+\infty} \frac{\mathcal{R}\{A(\omega')\}}{\omega - \omega'} d\omega' \tag{28}$$

it can be reconstructed. In practice $\mathcal{A}(p, \omega)$ is transformed back to time with a complex to complex Fourier transform $a_r(p, t) = \mathcal{F}_{\omega \to t}\{\mathcal{A}(p, \omega)\}$ and then the real part is taken.

Proof see [Bracewell, 1986]: A real signal $b(t)$ has a causal impulse response of

$$a(t) = H(t)b(t) \tag{29a}$$

$$a(t) = O(t) + E(t)(splitinevenandoddsignal) \tag{29b}$$

$$a(t) = \frac{1}{2}[a(t) + a(-t)] + \frac{1}{2}[a(t) - A(-t)] \tag{29c}$$

$$O(t) = sign(t)E(t) \tag{29d}$$

$$a(t) = (1 + sign(t))E(t) \tag{29e}$$

$$A(\omega) = G(\omega) + i(\frac{-2}{\omega}) * G(\omega) \tag{29f}$$

where $H(t)$ is the Heaviside step function:

$$H(t)\| = \begin{cases} 0 & t < 0 \\ \frac{1}{2} & t = 0 \\ 1 & t > 0 \end{cases} \tag{30}$$

2.2 Inverse model of Transmission response

Correlation of reflection matrix:

$$\mathbf{R}^H\mathbf{R} = \mathbf{L}\mathbf{\Lambda}_r\mathbf{L}^H \tag{31}$$

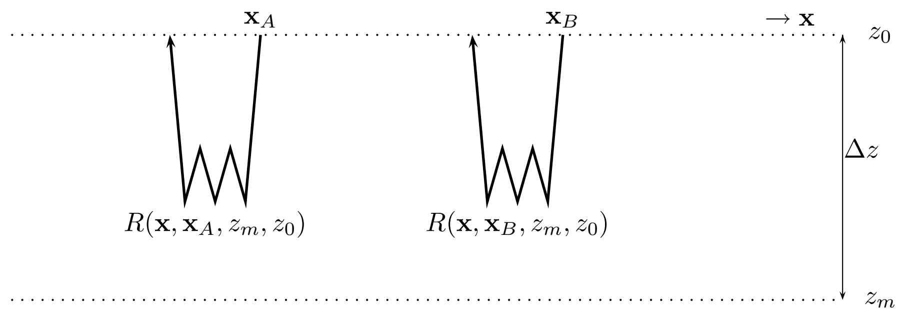

Flow diagram of computational tasks:

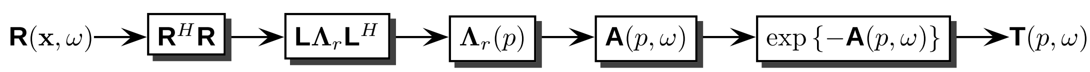

Details for different media:

$$\mathbf{R}^H\mathbf{R} = \begin{pmatrix} R^*(\mathbf{x}_{r,0}, \mathbf{x}_{s,0}) & \dots & R^*(\mathbf{x}_{r,M}, \mathbf{x}_{s,0}) \\ \vdots & \ddots & \vdots \\ R^*(\mathbf{x}_{r,0}, \mathbf{x}_{s,N}) & \dots & R^*(\mathbf{x}_{r,M}, \mathbf{x}_{s,N}) \end{pmatrix} \begin{pmatrix} R(\mathbf{x}_{r,0}, \mathbf{x}_{s,0}) & \dots & R(\mathbf{x}_{r,0}, \mathbf{x}_{s,N}) \\ \vdots & \ddots & \vdots \\ R(\mathbf{x}_{r,M}, \mathbf{x}_{s,0}) & \dots & R(\mathbf{x}_{r,M}, \mathbf{x}_{s,N}) \end{pmatrix} \quad (32a)$$

For a 1 dimensional medium this reduces to:

$$\mathbf{R}^H\mathbf{R} = \begin{pmatrix} R^*R(0) & \dots & R^*R(N) \\ \vdots & \ddots & \vdots \\ R^*R(N) & \dots & R^*R(0) \end{pmatrix} \quad (32b)$$

where R^*R is the auto-correlation function of the reflection response R. In the wavenumber domain $\mathbf{R}^H\mathbf{R}$ can be easily calculated using the Fourier transform of one shot record and compute the autocorralation in the wavenumber domain (in wavenumber domain all elements of the computation $l = re^2 + im^2$ are real).[Efficient algorithm for eigenvalue decomposition of Toeplitz matrix...., with circulant matrix as pre-conditioner.] The resulting cross-correlation matrix $\mathbf{R}^H\mathbf{R}$ in the spatial domain for 1D media is a Hermitian Toeplitz matrix (which has real eigenvalues, add proof for Hermitian matrix has real eigenvalues). Check that $\mathbf{R}^H\mathbf{R}$ has a diagonal with real elements.

$\mathbf{R}^H\mathbf{R}$ is a Circulant matrix for 1D sources (plane waves) in 1D media. The eigenvalues of a circulant matrix are obtained by taking the Fourier transform of the first column of $\mathbf{R}^H\mathbf{R}$ [Sjöström, 1996].

2.3 Eigenvalue decomposition of Complex matrices

The following programs can be used:

- standard LAPACK routine ZHEEVX() for Hermitian matrices
- standard LAPACK routine ZGEEV() solved via Schur-factorization
- use FFT for circulant matrices
- For Complex Symmetric Matrix routine of Victor Ryaboy (CS)

2.4 Symmetry relations of cross-correlation matrices

2D and 3D media with point(line) source:

$$(\mathbf{R}^H\mathbf{R})^H = \mathbf{R}^H\mathbf{R} \tag{33}$$
$$(\mathbf{R}^H\mathbf{R})^T = \mathbf{R}^T\mathbf{R}^* \tag{34}$$
$$(\mathbf{R}^H\mathbf{R})^* = \mathbf{R}^T\mathbf{R}^* \tag{35}$$

http://www.ee.ic.ac.uk/hp/staff/dmb/matrix/

2.4.1 Symmetric matrices

2.4.2 Hermitian matrices

A square matrix $\mathbf{A}$ is Hermitian if and only if $\mathbf{A} = \mathbf{A}^H$, that is $A(i,j) = A(j,i)^*$

For real matrices, Hermitian and symmetric are equivalent. Except where stated, the following properties apply to real symmetric matrices as well.

[Complex]: $\mathbf{A}$ is Hermitian if $x^H\mathbf{A}x$ is real for all (complex) x. The following are equivalent

- $\mathbf{A}$ is Hermitian and positive semidefinite
- A=BHB for some B
- $\mathbf{A} = \mathbf{C}^2$ for some Hermitian $\mathbf{C}$.

Any matrix A has a unique decomposition A = B + jC where B and C are Hermitian: B = (A+AH)/2 and C=(A-AH)/2j Hermitian matrices are closed under addition, multiplication by a scalar, raising to an integer power, and (if non-singular) inversion. The eigenvalues of a Hermitian matrix are all real. Hermitian matrices are normal A is Hermitian iff xHAy=xHAHy for all x and y. If A and B are hermitian then so are AB+BA and j(AB-BA) where j =sqrt(-1). For any complex a with —a—=1, there is a 1-to-1 correspondence between the unitary matrices, U, not having a as an eigenvalue and hermitian matrices, H, given by U=a(jH-I)(jH+I)-1 and H=j(U+aI)(U-aI)-1 where j =sqrt(-1). These are Caley's formulae.

Taking a=-1 gives U=(I-jH)(I+jH)-1=(I+jH)-1(I-jH) and H=j(U-I)(U+I)-1=j(U+I)-1(U-I).

2.4.3 Toeplitz matrices

A toeplitz matrix, A, has constant diagonals. In other words ai,j depends only o
If A=TOE(b[m+n-1])[m#n] then ai,j = bi-j+n.
In the topics below, J is the exchange matrix.

A toeplitz matrix is persymmetric and so, if it exists, is its inverse. A symmet
If A and B are toeplitz, then so are A+B and A-B. Note that AB and A-1 are not n
If A is toeplitz, then AT, AH and JAJ are Toeplitz while JA, ATJ, AJ and JAT are

If A[n#n] is toeplitz, then JATJ=(JAJ)T=A while JA=ATJ and AJ=JAT are Hankel.

TOE(a+b) = TOE(a) + TOE(b)
TOE(b[m+n-1])[m#n]=TOE(Jb)[n#m]T

TOE(b[2n-1])[n#n]=TOE(Jb)[n#n]T

If the lower triangular matrices A[n#n]=TOE([0[n-1]; p[n]]) and B[n#n]=TOE([0[n-

Aq = Bp = conv(p,q)1:n

AB = BA = TOE([0[n-1]; Aq]) = TOE([0[n-1]; Bp]) = TOE([0[n-1]; conv(p,q)1:n])

A-1 and B-1 are toeplitz lower triangular if they exist.

If the upper triangular matrices A[n#n]=TOE([p[n]; 0[n-1]]) and B[n#n]=TOE([q[

Aq = Bp = conv(p,q)n:2n-1

AB = BA = TOE([Aq; 0[n-1]]) = TOE([Bp; 0[n-1]]) = TOE([conv(p,q)n:2n-1; 0[n-1]])

A-1 and B-1 are toeplitz lower triangular if they exist.

The product TOE(a)[m#r]TOE(b)[r#n] is toeplitz iff ar+1:r+m-1b1:n-1T = a1:m-1br+

TOE(a)[m#r]TOE(b)[r#n] is toeplitz if ar+1:r+m-1 = a1:m-1 and br+1:r+n-1= b1:n-1
TOE([0[m-1]; a[r]])[m#r]TOE([0[n-1]; b[r]])[r#n] = TOE([0[n+m-r-1]; conv(a,b)1:r
TOE([a[r]; 0[m-1]])[m#r]TOE([b[r]; 0[n-1]])[r#n] = TOE([conv(a,b)r:2r-1; 0[n+m-

If A=TOE(b)[m#n] then JAJ=TOE(Jb)[m#n]
TOE([0[n-p]; a[m]; 0[q-m]])[q-p+1#n] b[n] = TOE([0[m-p]; b[n]; 0[q-n]])[q-p+1#m]

TOE(a[m])[m-n+1#n] b[n] = conv(a,b)n:m
TOE([0[n-p]; a[n]])[n-p+1#n] b[n] = TOE([0[n-p]; b[n]])[n-p+1#n] a[n] = conv(a,b

TOE([0[n-1]; a[n]])[n#n] b[n] = TOE([0[n-1]; b[n]])[n#n] a[n] = conv(a,b)1:n

```
TOE([a[n]; 0[q-n]])[q-n+1#n] b[n] = TOE([b[n]; 0[q-n]])[q-n+1#n] a[n] = conv(a,b

TOE([a[n]; 0[n-1]])[n#n] b[n] = TOE([b[n]; 0[n-1]])[n#n] a[n] = conv(a,b)n:2n-1

TOE([0[n-1]; a[m]; 0[n-1]])[m+n-1#n] b[n] = TOE([0[m-1]; b[n] ;0[m-1]])[m+n-1#m]

A symmetric toeplitz matrix is of the form S[n#n] = TOE([Ja[n]; 0[n-1]]+[0[n-1];

JSJ = S
Sb = (TOE([b[n]; 0[n-1]])[n#n]J+TOE([0[n-1]; b[n]])[n#n])a . The matrix on the r
```

2.4.4 Circulant matrices

A Circular matrix, A, is one for which inv(A) = conj(A). A matrix A is circular iff A=exp (j B) where j = sqrt(-1), B is real and exp() is the matrix exponential function. If A = B + jC where B and C are real and j = sqrt(-1) then A is circular iff BC=CB and also BB + CC = I.

A circulant matrix is a square Toeplitz matrix with the additional cyclic property. An $m \times n$ Toeplitz matrix has at most $m = n - 1$ distinct elements, a circulant matrix has at most m distinct elements. A matrix-vector product with an $m \times n$ Toeplitz or Hankel matrix can be computed via the FFT.

Any circulant matrix can be diagonalized by the DFT matrix. A matrix-vector product with a circulant matrix can be computed via the eigenvalue decomposition and the FFT. Three DFT (forward and backward) are needed.

Any circulant matrix

$$\mathbf{C} = \begin{pmatrix} c_0 & c_{n-1} & c_{n-2} & \dots & c_1 \\ c_1 & c_0 & c_{n-1} & \dots & c_2 \\ c_2 & c_1 & c_0 & \dots & c_3 \\ \vdots & \vdots & \vdots & & \vdots \\ c_{n-1} & c_{n-2} & c_{n-3} & \dots & c_0 \end{pmatrix}$$

can be diagonalized by the DFT matrix.

$$\mathbf{\Lambda} = \mathbf{F}\mathbf{C}\mathbf{F}^H$$

The eigenvalues of **C** are the discrete Fourier transform of the first column in **C**.

Example, 4×4 circulant matrix:

$$\mathbf{C} = \begin{pmatrix} a & b & c & d \\ d & a & b & c \\ c & d & a & b \\ b & c & d & a \end{pmatrix} \quad (36)$$

An $m \times n$ Toeplitz matrix can be embedded in a circulant matrix of order $m+n$ or smaller.
A $m \times n$ Toeplitz matrix

$$\mathbf{T} = \begin{pmatrix} x_m & x_{m+1} & & \cdots & x_{m+n-1} \\ x_{m-1} & x_m & x_{m+1} & & \vdots \\ \vdots & x_{m-1} & x_m & \ddots & \vdots \\ \vdots & & x_{m-1} & \ddots & x_{m+1} \\ \vdots & & & \ddots & x_m \\ \vdots & & & & x_{m-1} \\ \vdots & & & & \vdots \\ x_1 & & & & x_n \end{pmatrix}$$

can be represented by

$$T_{col} = \begin{pmatrix} x_m \\ x_{m-1} \\ \vdots \\ x_1 \end{pmatrix}, T_{row} = \begin{pmatrix} x_{m+n-1} \\ x_{m+n-2} \\ \vdots \\ x_{m+1} \end{pmatrix}$$

First column of circulant matrix has the form:

$$C = \begin{pmatrix} T_{col} \\ 0 \\ T_{row} \end{pmatrix} \tag{37}$$

Example 3×3 Toeplitz

$$\mathbf{T} = \begin{pmatrix} x_3 & x_4 & x_5 \\ x_2 & x_3 & x_4 \\ x_1 & x_2 & x_3 \end{pmatrix} \tag{38}$$

$$T_{col} = \begin{pmatrix} x_3 \\ x_2 \\ x_1 \end{pmatrix}, T_{row} = \begin{pmatrix} x_5 \\ x_4 \end{pmatrix} \tag{39}$$

$$C^T = (x_3, x_2, x_1, 0, 0, 0, x_5, x_4) \tag{40}$$

$$
\mathbf{C} = \begin{pmatrix}
x_3 & x_4 & x_5 & 0 & 0 & 0 & x_1 & x_2 \\
x_2 & x_3 & x_4 & x_5 & 0 & 0 & 0 & x_1 \\
x_1 & x_2 & x_3 & x_4 & x_5 & 0 & 0 & 0 \\
0 & x_1 & x_2 & x_3 & x_4 & x_5 & 0 & 0 \\
0 & 0 & x_1 & x_2 & x_3 & x_4 & x_5 & 0 \\
0 & 0 & 0 & x_1 & x_2 & x_3 & x_4 & x_5 \\
x_5 & 0 & 0 & 0 & x_1 & x_2 & x_3 & x_4 \\
x_4 & x_5 & 0 & 0 & 0 & x_1 & x_2 & x_3
\end{pmatrix} \tag{41}
$$

Note that correlation matrices are Hermitian:

$$
\begin{aligned}
(\mathbf{T}^H\mathbf{T})^H &= \mathbf{T}^H\mathbf{T} \\
(\mathbf{T}^H\mathbf{T})^* &= \mathbf{T}^T\mathbf{T}^* = \mathbf{T}^*\mathbf{T}^T = (\mathbf{T}^H\mathbf{T})^T \\
(\mathbf{T}^T\mathbf{T}^*)^T &= \mathbf{T}^H\mathbf{T}
\end{aligned}
$$

Proof that Hermitian matrix has real eigenvalues.

example circulant matrix() 3 layer medium 1000-4000-1000 m/s thickness 100 m

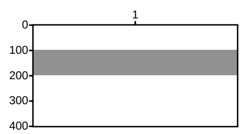

a. Model.

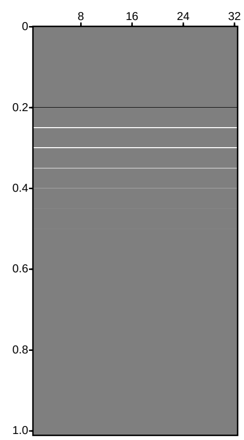

b. Reflection data

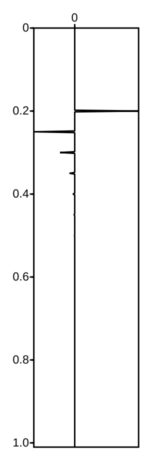

c. Reflection trace

Figure 1: Circulant matrices: plane wave in 1D medium.

$$\mathbf{R}^H\mathbf{R} = \mathbf{L}\mathbf{\Lambda}_r\mathbf{L}^H$$

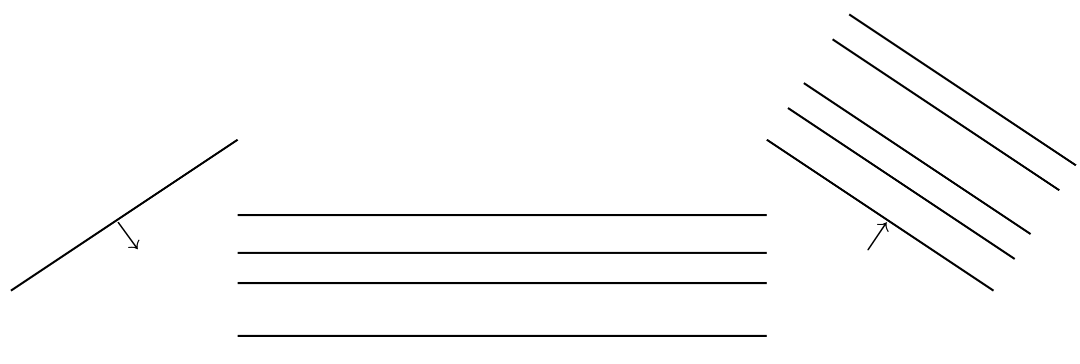

Figure 2: Eigenvectors interpreted as plane waves.

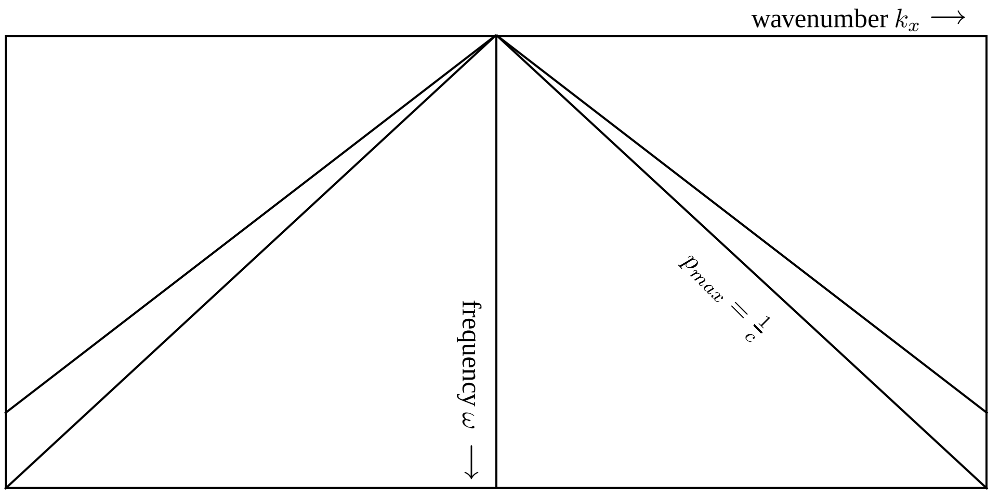

Figure 3: .

2.5 Eigenvalues of Hermitian matrices

Using program based on [Bar-On and Ryaboy, 1997]

Problem: "How to make sure that the calculated eigenvalues correspond to k_x values which are known?' analysis of eigenvectors.

example for rescaling from k_x to ray-parameter. Scaling from wavenumber k_x to ray-parameter p with $\frac{1}{\omega}(k_x = p\omega)$.

Following equation (4) and equation (18).

$$\mathbf{C}^H\mathbf{C} = \mathbf{I} - \mathbf{R}^H\mathbf{R} \tag{42a}$$
$$\mathbf{C}^H\mathbf{C} = \mathbf{I} - \mathbf{L}\mathbf{\Lambda}_r\mathbf{L}^H \tag{42b}$$
$$\mathbf{L}\mathbf{\Lambda}_c^H\mathbf{\Lambda}_c\mathbf{L}^H = \mathbf{L}[\mathbf{I} - \mathbf{\Lambda}_r]\mathbf{L}^H \tag{42c}$$
$$\exp\{-2\Re\{\underset{\sim}{\mathbf{A}}\}\Delta z_{tot}\} = \mathbf{I} - \mathbf{\Lambda}_r \tag{42d}$$
$$\Re[\underset{\sim}{\mathbf{A}}] = -\frac{1}{2\Delta z_{tot}}\ln\{\mathbf{I} - \mathbf{\Lambda}_r\} \tag{42e}$$

Alternative:

$$\mathbf{C}^H\mathbf{C} = \mathbf{I} - \mathbf{R}^H\mathbf{R} \tag{43a}$$
$$\mathbf{C}^H\mathbf{C} = \mathbf{L}\mathbf{\Lambda}_r'\mathbf{L}^H \tag{43b}$$

where $\mathbf{\Lambda}_r'$ are the eigenvalues of $\mathbf{I} - \mathbf{R}^H\mathbf{R}$.

Practical problems:

- Computation of $\mathbf{I} - \mathbf{R}^H\mathbf{R}$
- Eigenvector analysis for 2D media
- Ordering of eigenvalues (per ω) and mapping to k_x, zero-crossing to order the eigenvectors.
- Check eigenvectors: $\mathbf{L}^H\mathbf{L} = \mathbf{I}$ or equal to scaling matrix (=diagonals contain scale factors)
- Correct scaling of amplitudes: Δx factor
- Windowing of R; below $\partial\mathcal{D}$ heterogeneous media
- Construction of W_g from C and W_p
- Spectrum of coda operator should be flat (does not contain $\frac{1}{\omega}$ trend)
- check $\mathbf{R}^H\mathbf{R}$ has real diagonal

For a one dimensional medium $\underset{\sim}{\mathbf{\Lambda}}_c$ is the spatial Fourier transform of $\mathbf{C}$.

$$\tilde{C}(k_x, \mathbf{x}_a, \omega) = \int_{-\infty}^{\infty} C(\mathbf{x}, \mathbf{x}_a, \omega) \exp\left(-jk_x\mathbf{x}\right) d\mathbf{x} \tag{44}$$

where $\tilde{C}$ denotes the wavenumber domain.

Show the relation between eigenvalues (plane waves) and Fourier transform. Fourier transform is eigenvalue decomposition of the (one-way) wave equation operator?......

2.6 Alternative (Martijn)

$$\mathbf{C}^H\mathbf{C} = \mathbf{I} - \mathbf{R}^H\mathbf{R} \tag{45a}$$

$$\mathbf{F}\mathbf{C} = \mathbf{I} \tag{45b}$$

$$\mathbf{C}^H\mathbf{C}[\mathbf{I} - \mathbf{R}^H\mathbf{R}]^-1 = \mathbf{I} \tag{45c}$$

$$\mathbf{F} = \mathbf{C}^H[\mathbf{I} - \mathbf{R}^H\mathbf{R}]^-1 \tag{45d}$$

3 Computational steps

4 Numerical Experiments in 2D

Flux normalized operators must be used.

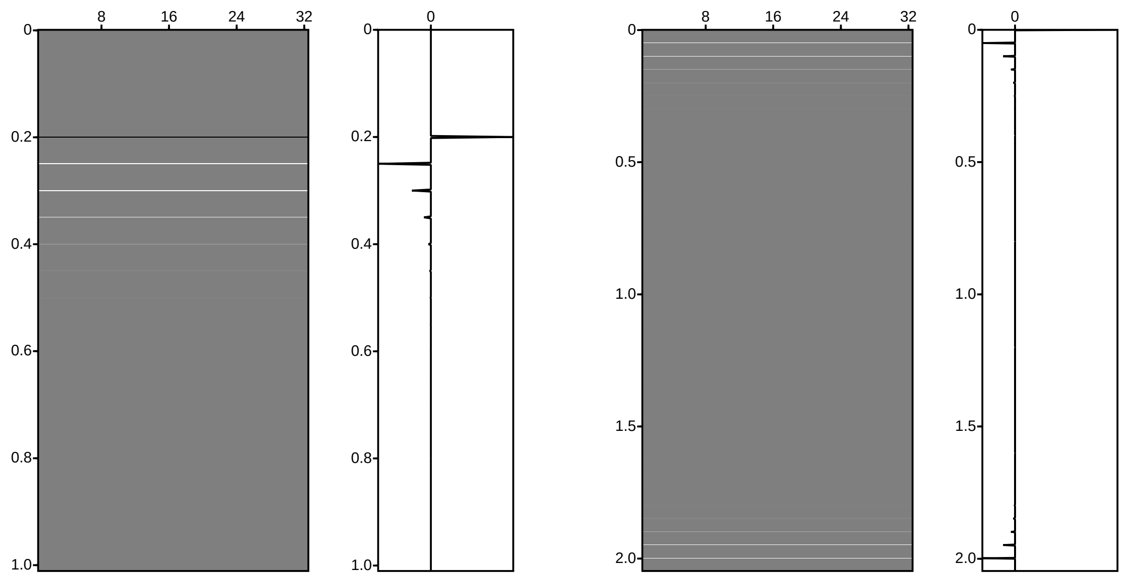

shot-record $\mathbf{R}$ auto-correlation $\mathbf{R}^H\mathbf{R}$

Figure 4: Plane waves in 1D medium.

4.1 2D examples 1D medium

4.1.1 plane wave in 1D medium (1 Dimensional experiment)

$\mathbf{R}^H\mathbf{R}$ is a Circulant matrix for 1D sources (plane waves) in 1D media. The eigenvalues of a circulant matrix are obtained by taking the Fourier transform of the first column, so $A_l(\omega) = \tilde{\mathcal{A}}_l(k_{x,l}, \omega)$.

3 layer medium 1000-4000-1000 m/s thickness 100 m: $4000/200 = 0.05$ s. internal multiple train.

$\mathbf{R}^H\mathbf{R}$ is a Hermitian matrix for a fixed spread geometry.

See paper Kees: plane wave experiments

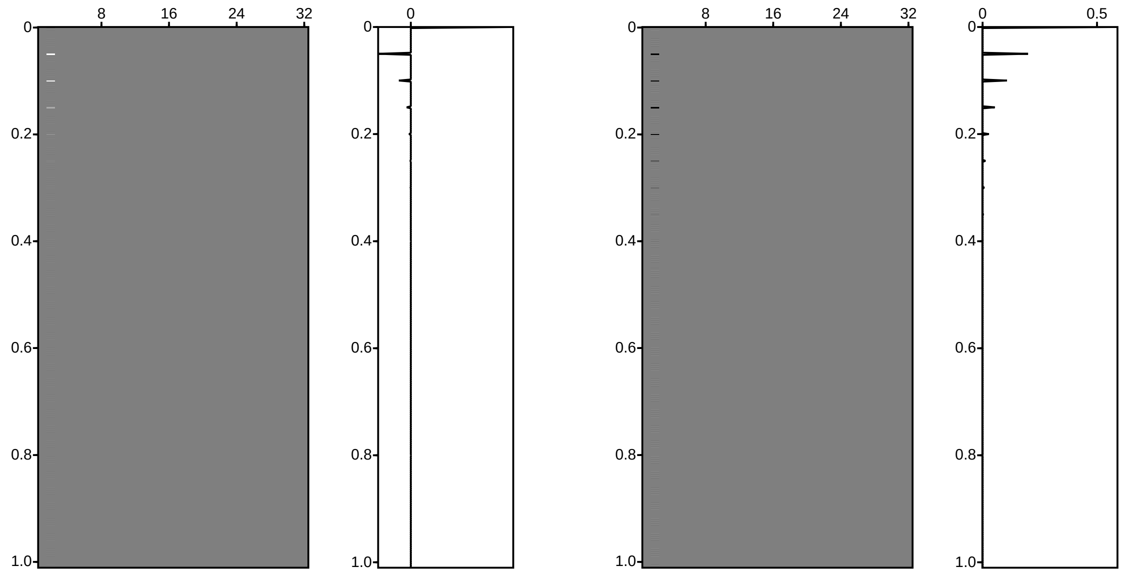

diagonal $\mathbf{\Lambda}_r$ 2'nd trace   coda **C**

Figure 5: Eigenvalues calculated with Lapack routine.

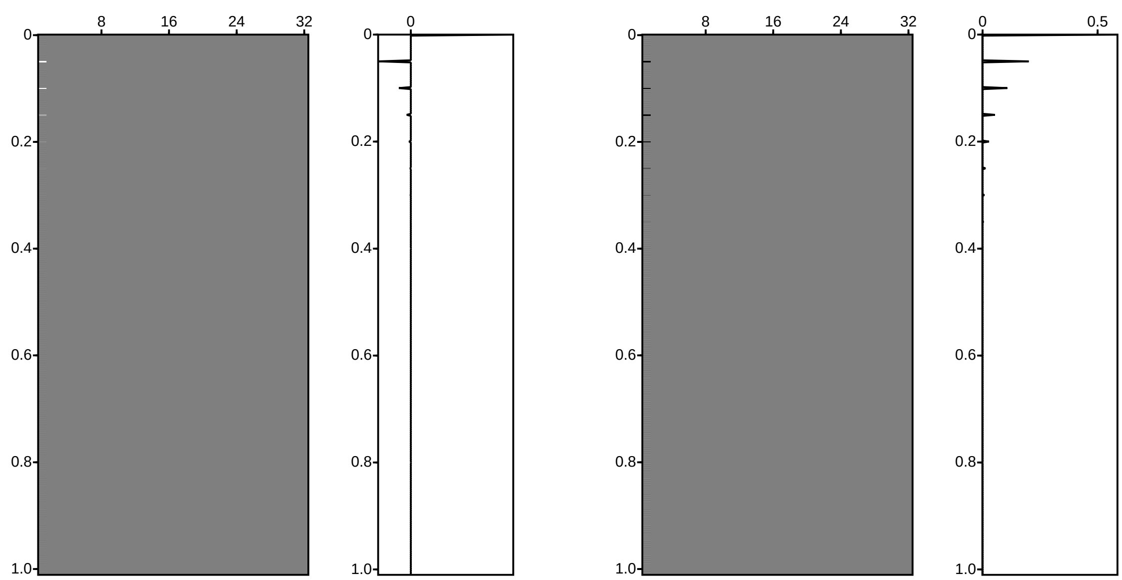

diagonal $\mathbf{\Lambda}_r$ 1'st trace   coda **C**

Figure 6: Eigenvalues calculated with FFT routine.

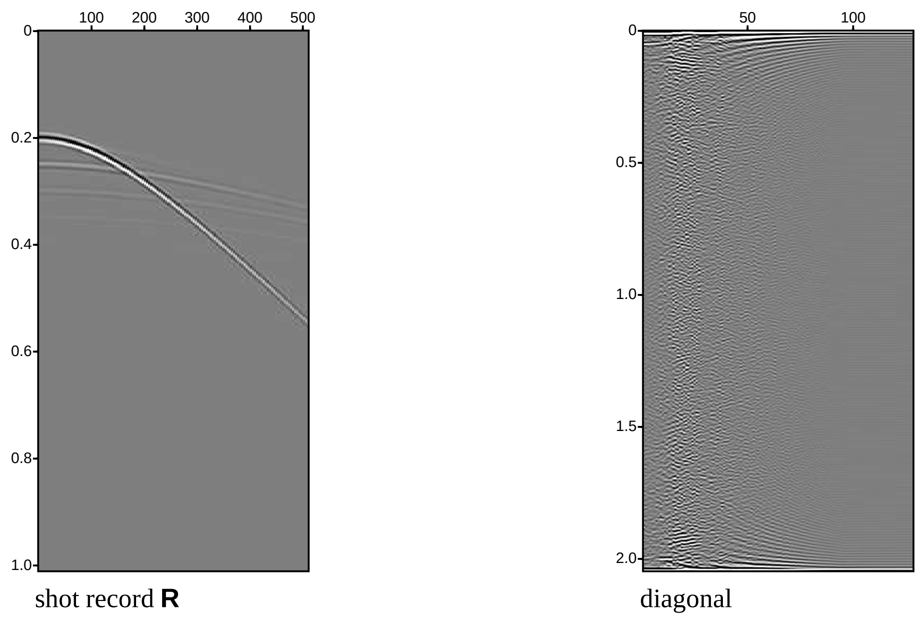

Figure 7: Eigenvalues calculated with Lapack routine; Point source.

4.1.2 Line source in 1D medium: reflection data

3 layer medium 1000-4000-1000 m/s thickness 200 m: $4000/400 = 0.1$ s. internal multiple train.

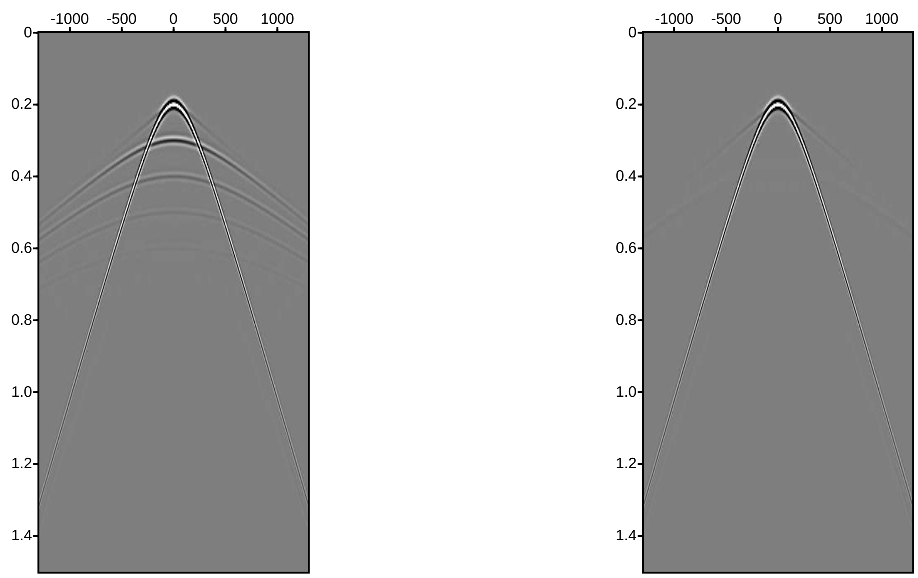

shot record $\mathbf{R}$ shot record $\mathbf{R}_1$

Figure 8: Reflection responses with and without internal multiples.

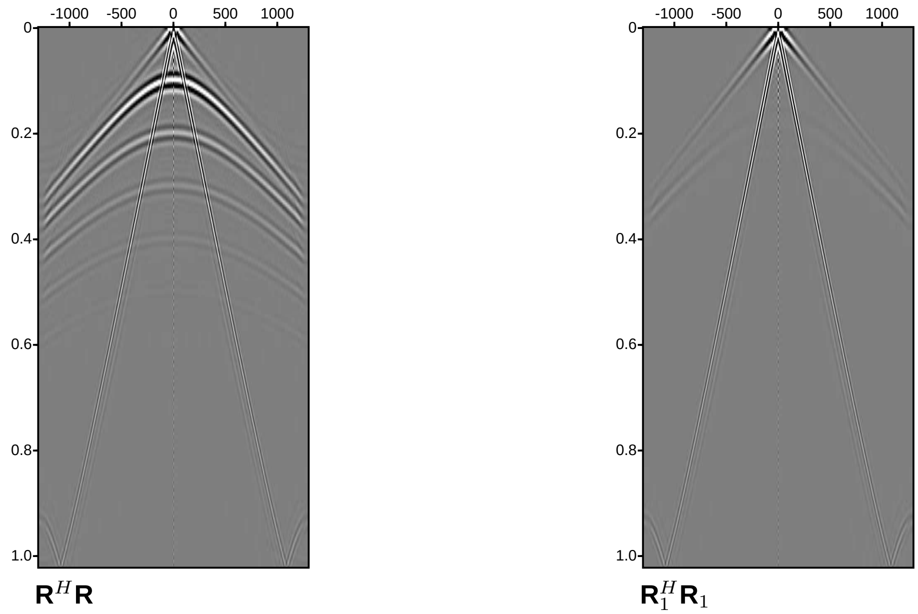

Figure 9: Correlations of reflection responses.

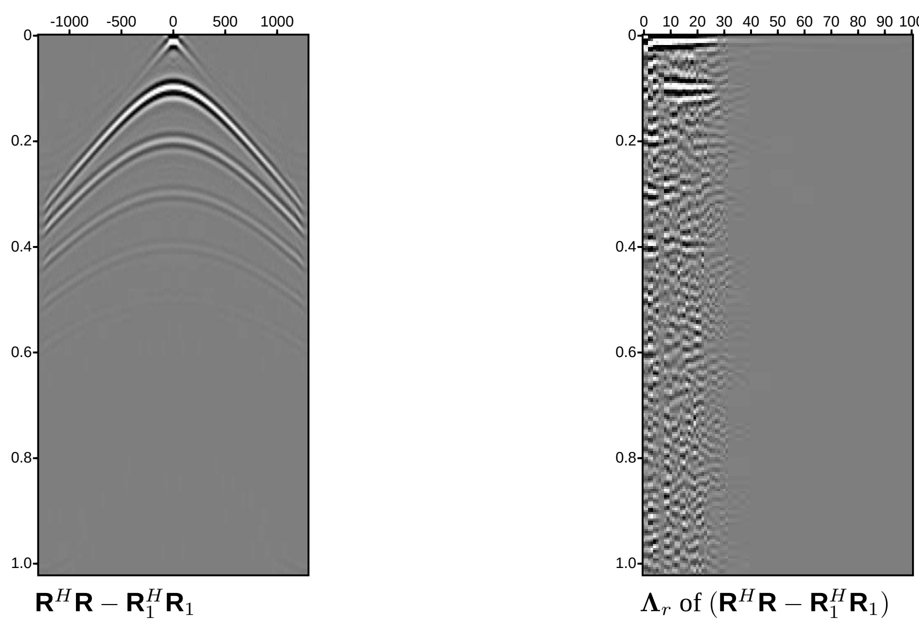

Figure 10: Difference of correlations and eigenvalues of the correlation difference

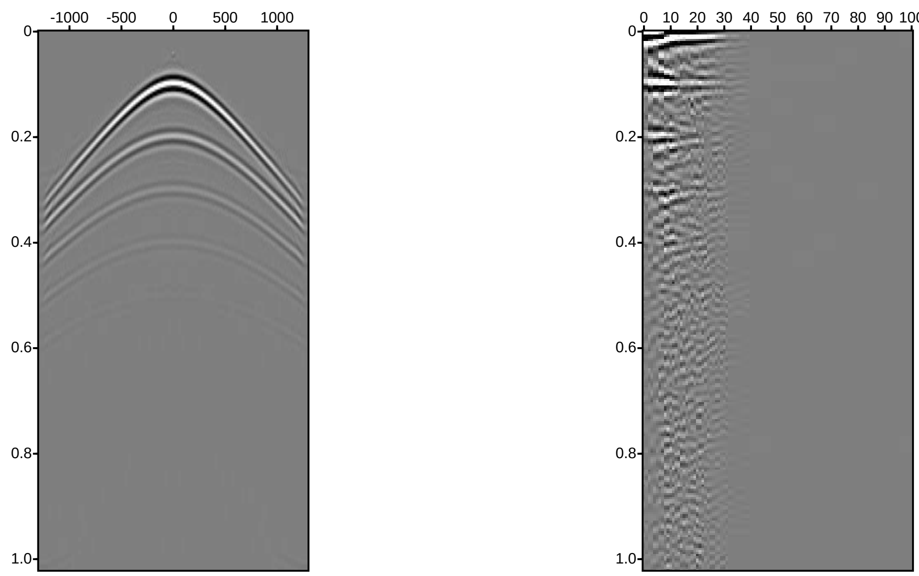

$\mathbf{R}^H\mathbf{R}$ muted for direct field

$\mathbf{\Lambda}_r$ of $\mathbf{R}^H\mathbf{R}$ muted

Figure 11: Difference of correlations and eigenvalues of the correlation difference muted for direct field.

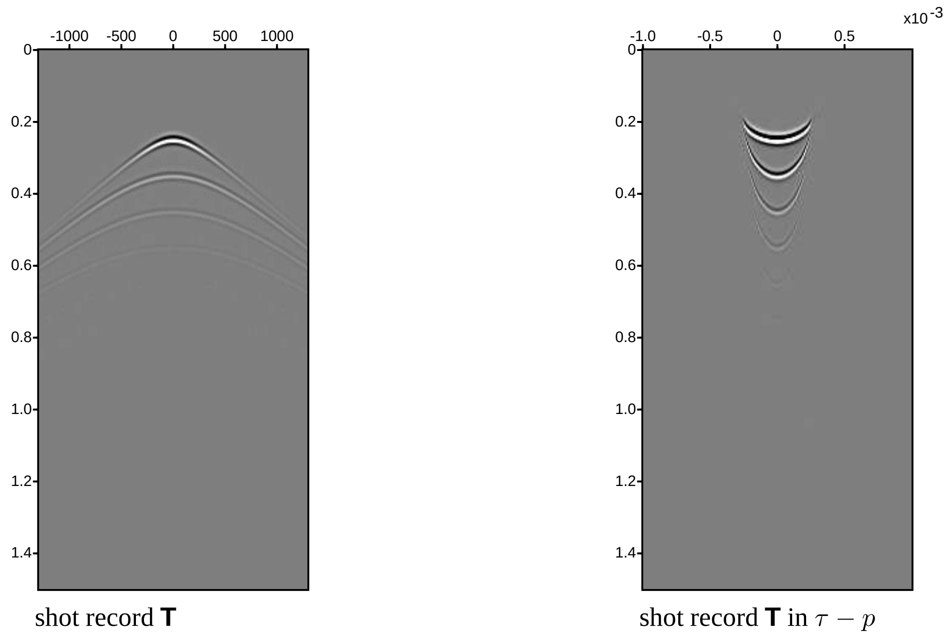

Figure 12: Transmission response in $x - t$ and $\tau - p$ domain.

4.1.3 Line source in 1D medium: transmission data

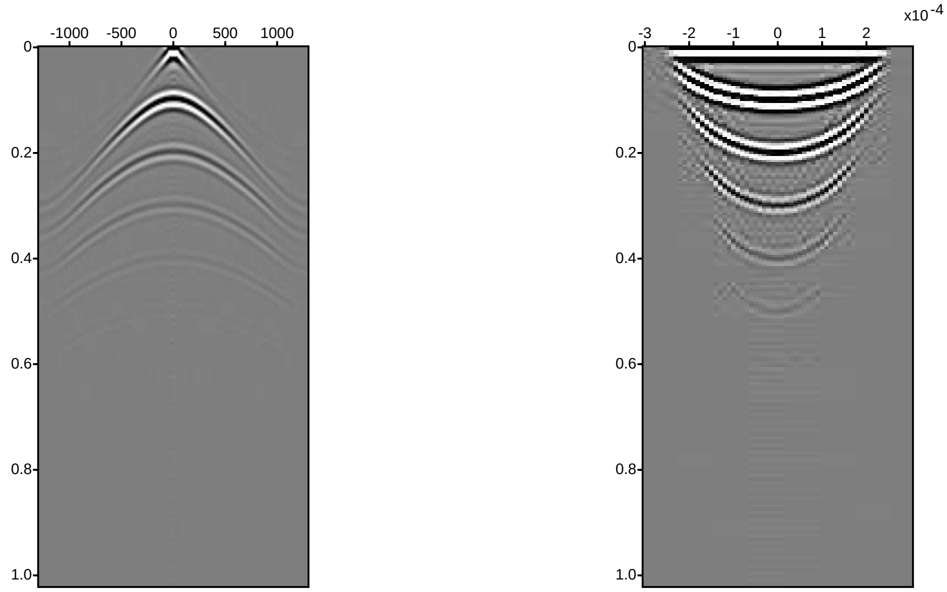

$\mathbf{T}^H\mathbf{T}$ in $x - t$ $\quad$ $\mathbf{T}^H\mathbf{T}$ in $\tau - p$

Figure 13: correlation of transmission response in $x - t$ and $\tau - p$ domain.

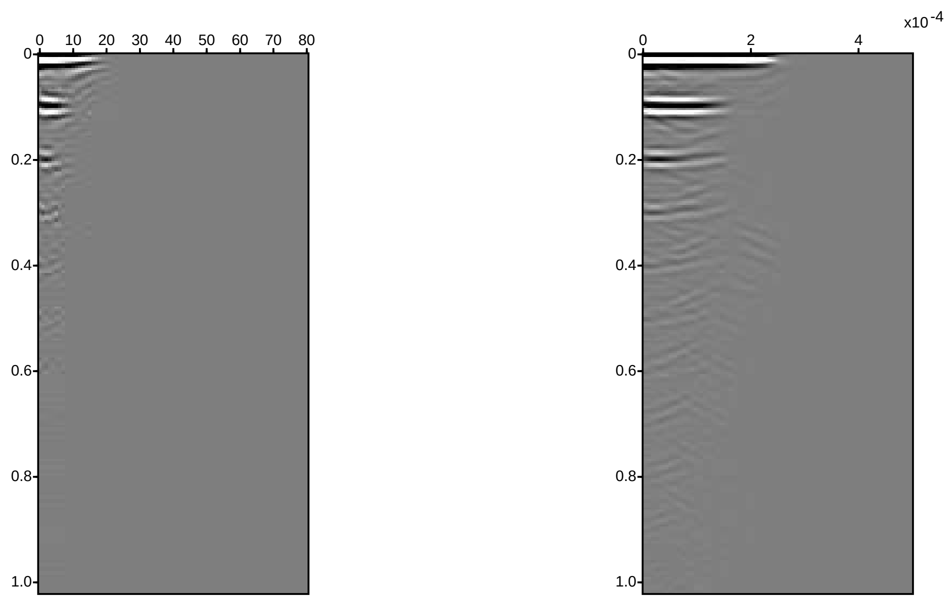

$\mathbf{\Lambda}_t$ of $\mathbf{T}^H\mathbf{T}$ in $k_x - t$ $\quad$ $\mathbf{\Lambda}_t$ of $\mathbf{T}^H\mathbf{T}$ in $\tau - p$

Figure 14: Eigenvalues of correlation of transmission response in $\tau - p$ domain with LAPACK routines. time 444 seconds

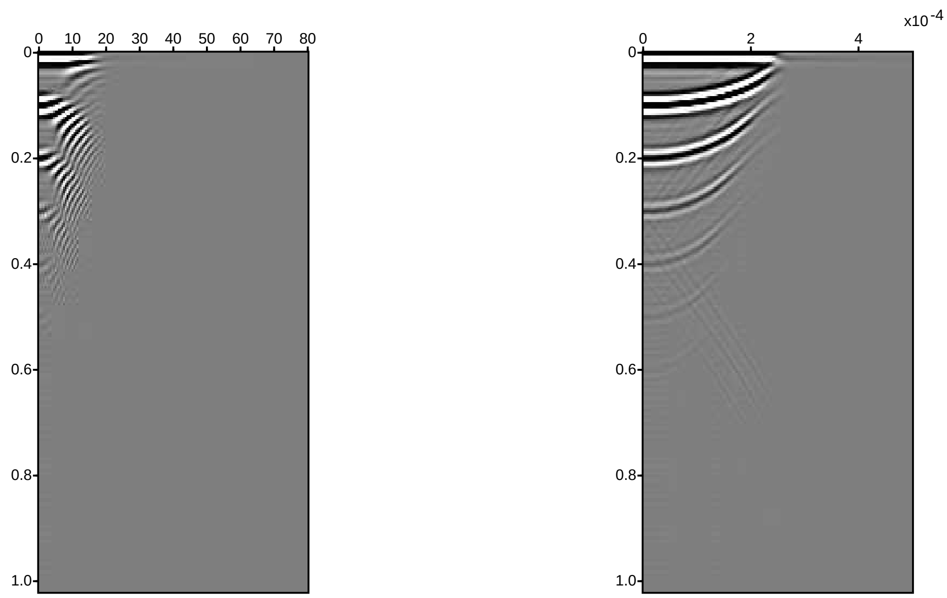

$\mathbf{\Lambda}_t$ of $\mathsf{T}^H\mathsf{T}$ in $k_x - t$ $\mathbf{\Lambda}_t$ of $\mathsf{T}^H\mathsf{T}$ in $\tau - p$

Figure 15: Eigenvalues of correlation of transmission response in $\tau - p$ domain with FFT's using Circular matrix. time 6 seconds

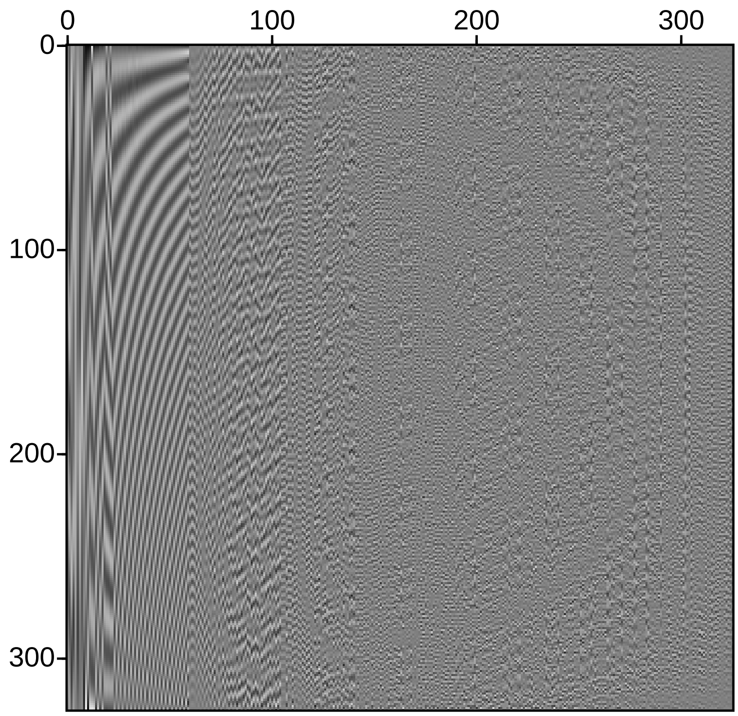

Figure 16: Real part of eigenVectors of $\mathbf{T}^H\mathbf{T}$ for frequency plane 30 (15 Hz). Vertical is the eigenvector length, horizontal the eigenvector number.

4.1.4 Line source in 1D medium: eigenvectors

Problem: ”How to make sure that the calculated eigenvalues correspond to k_x values which are known?’ analysis of eigenvectors.

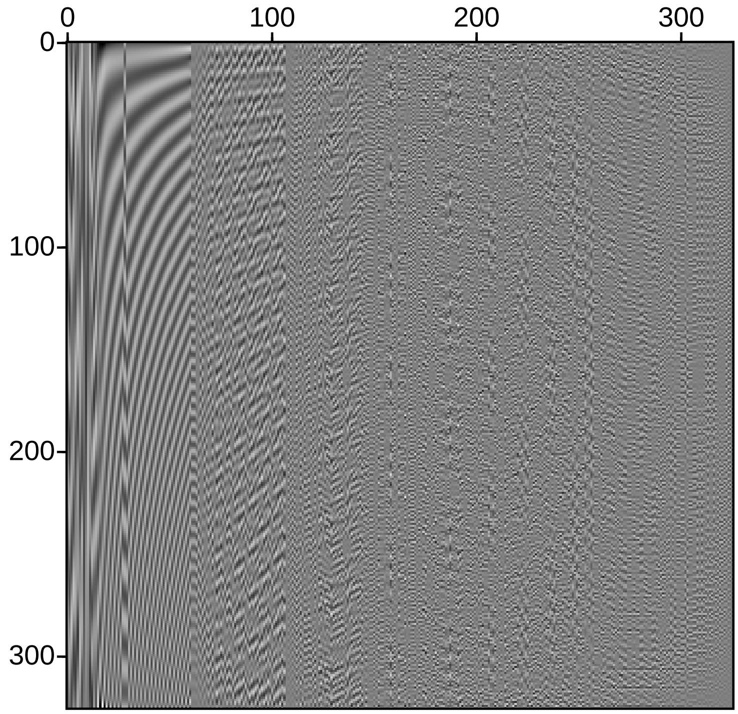

Figure 17: Real part of eigenVectors of $\mathbf{T}^H\mathbf{T}$ for frequency plane 50 (25 Hz). Vertical is the eigenvector length, horizontal the eigenvector number.

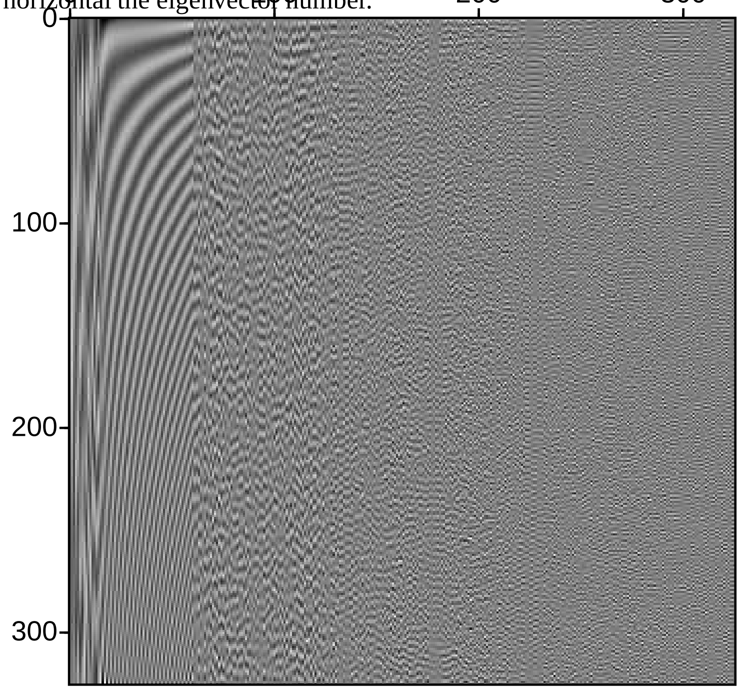

Figure 18: Sorted eigenVectors of $\mathbf{T}^H\mathbf{T}$ for frequency plane 50 (25 Hz). Vertical is the eigenvector length, horizontal the eigenvector number.

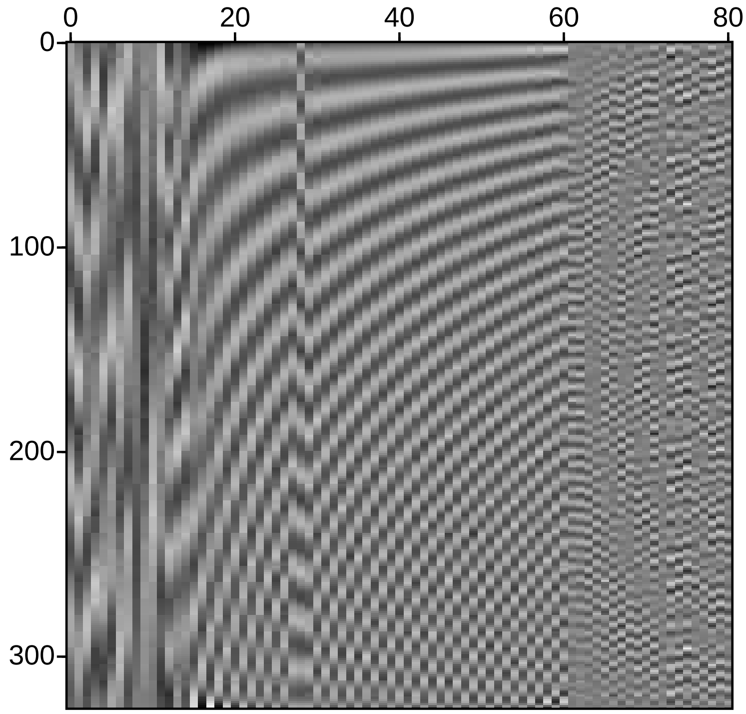

Figure 19: Zoom of real part of eigenVectors of $\mathbf{T}^H\mathbf{T}$ for frequency plane 50 (25 Hz). Vertical is the eigenvector length, horizontal the eigenvector number.

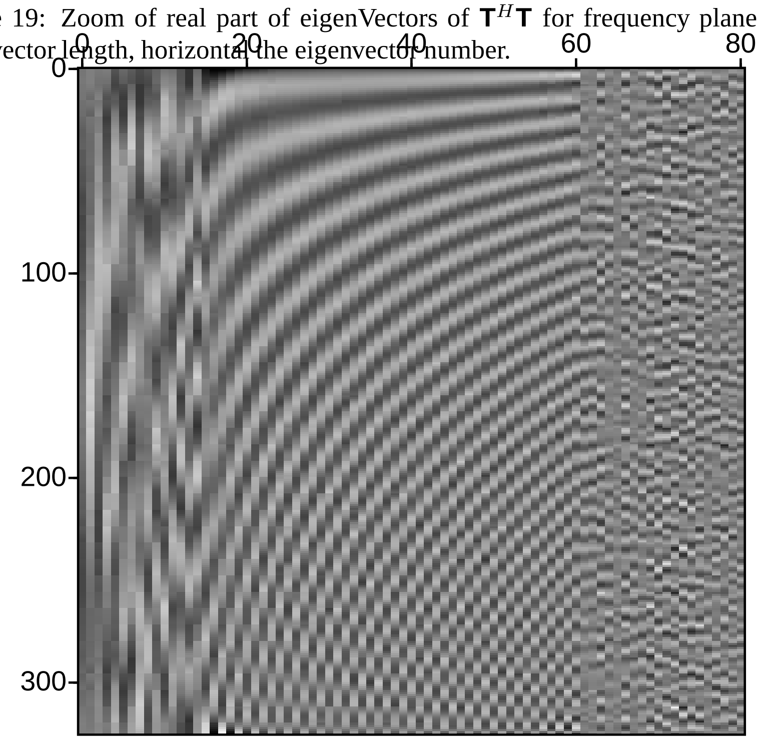

Figure 20: Sorted eigenVectors of $\mathbf{T}^H\mathbf{T}$ for frequency plane 50 (25 Hz). Vertical is the eigenvector length, horizontal the eigenvector number.

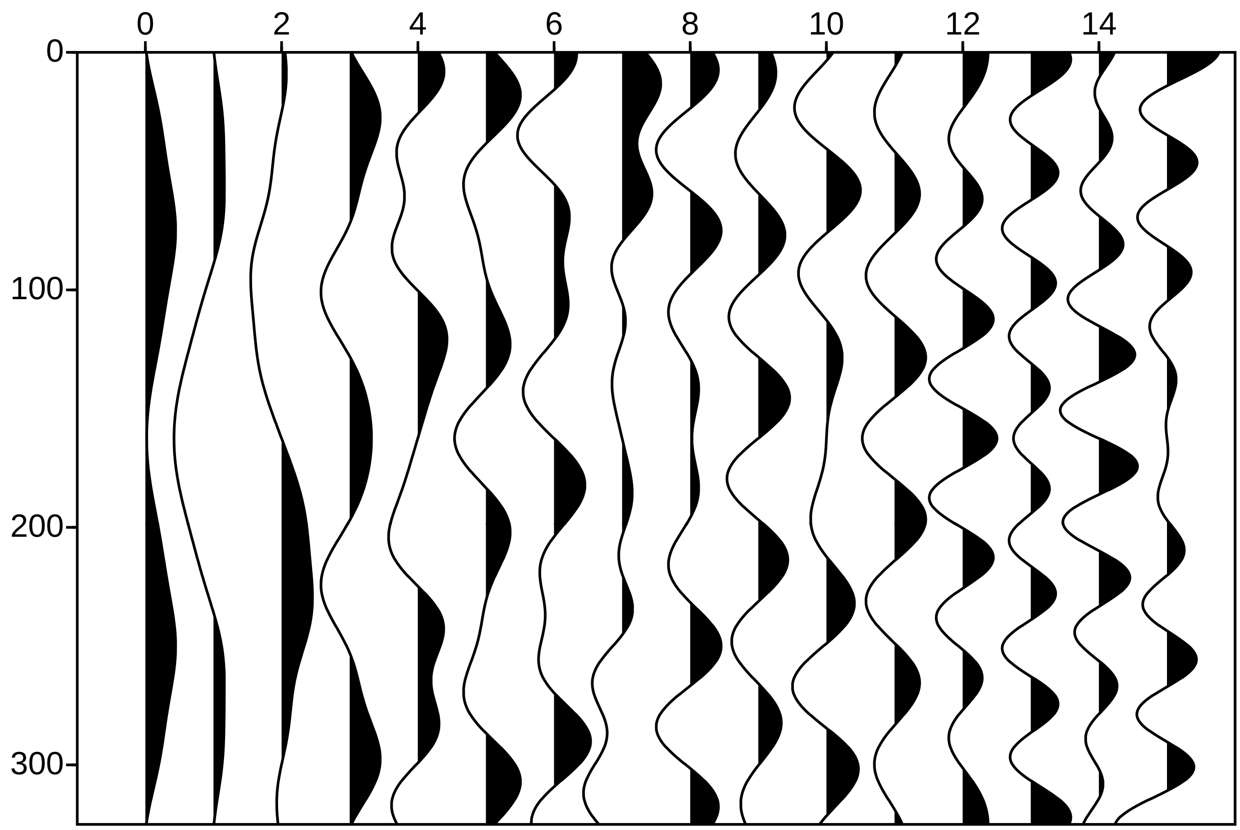

Figure 21: Sorted eigenVectors of $\mathbf{T}^H\mathbf{T}$ for frequency plane 50 (25 Hz). Vertical is the eigenvector length, horizontal the eigenvector number.

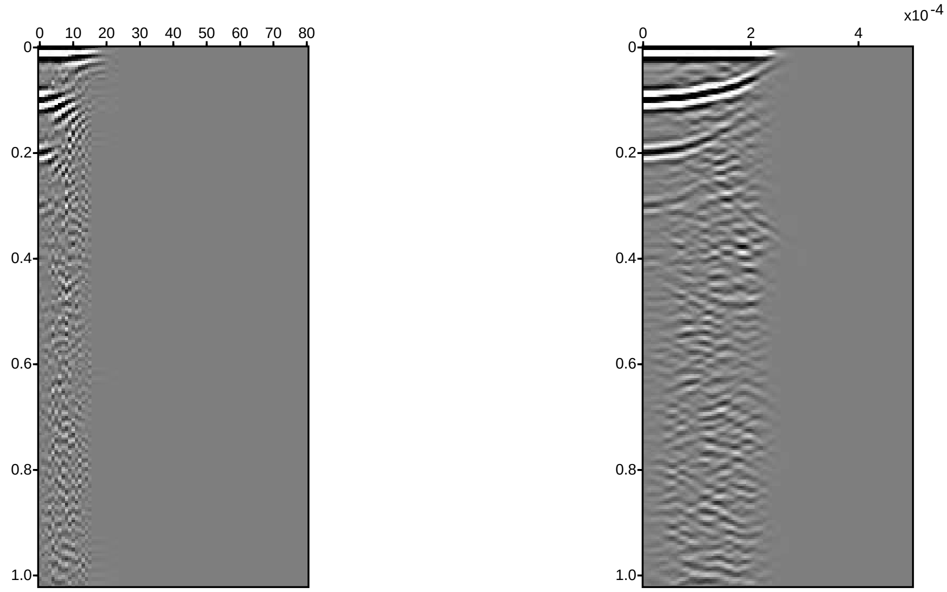

$\mathbf{\Lambda}_t$ of $\mathbf{T}^H\mathbf{T}$ in $k_x - t$ $\mathbf{\Lambda}_t$ of $\mathbf{T}^H\mathbf{T}$ in $\tau - p$

Figure 22: Sorted eigenvalues of correlation of transmission response in $\tau - p$ domain with LAPACK routines. time

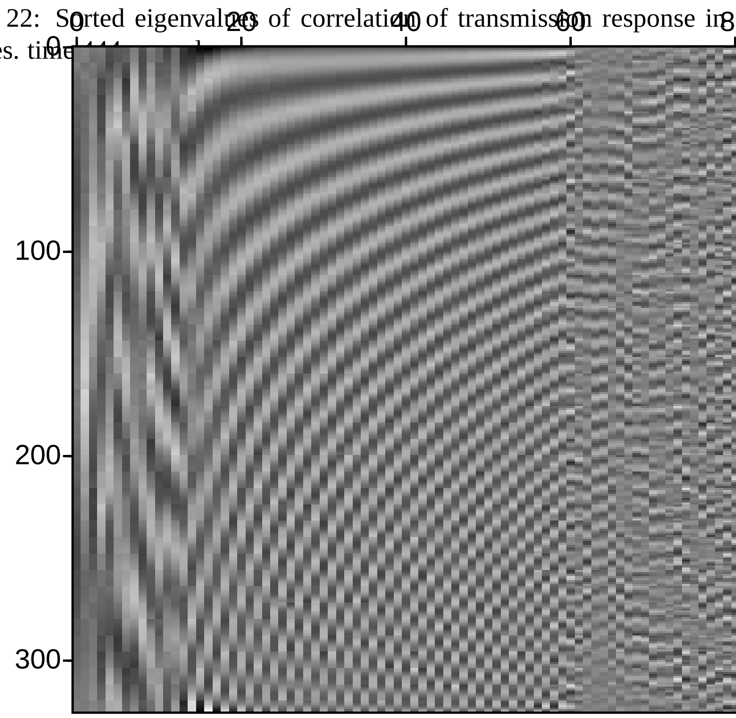

Figure 23: Sorted eigenVectors based on frequency content of $\mathbf{T}^H\mathbf{T}$ for frequency plane 50 (25 Hz). Vertical is the eigenvector length, horizontal the eigenvector number.

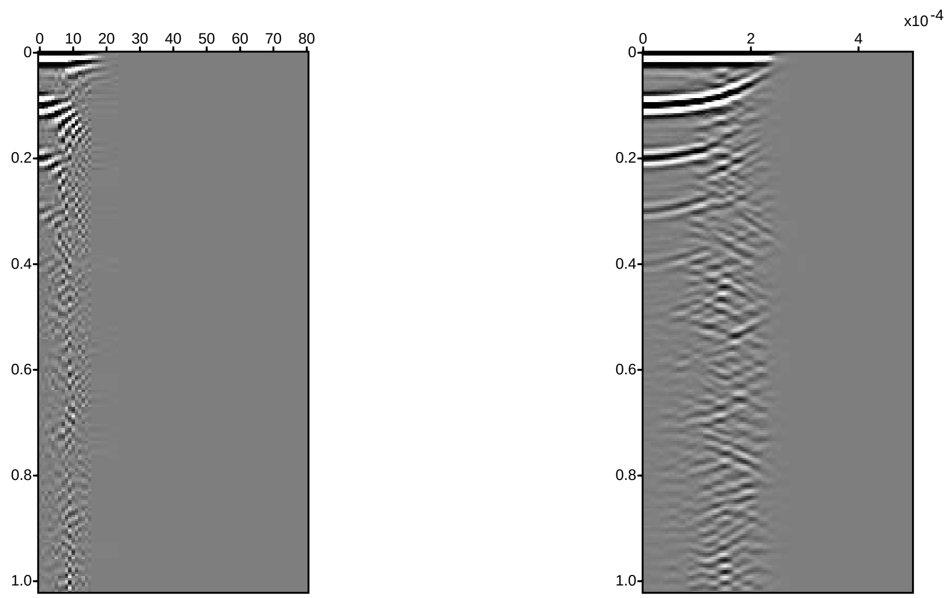

$\mathbf{\Lambda}_t$ of $\mathsf{T}^H\mathsf{T}$ in $k_x - t$ $\quad$ $\mathbf{\Lambda}_t$ of $\mathsf{T}^H\mathsf{T}$ in $\tau - p$

Figure 24: Sorted eigenvalues based on frequency content of correlation of transmission response in $\tau - p$ domain with LAPACK routines. time 444 seconds

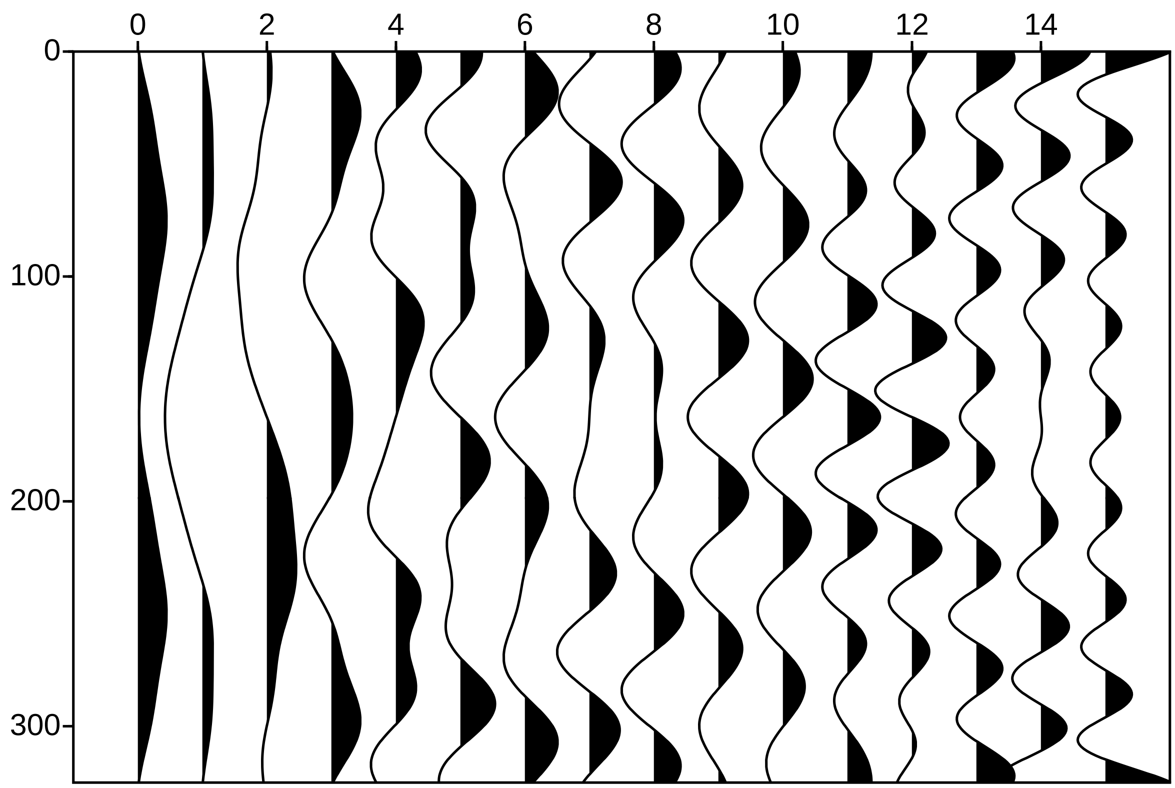

Figure 25: Sorted eigenVectors based on frequency content of $\mathbf{T}^H\mathbf{T}$ for frequency plane 50 (25 Hz). Vertical is the eigenvector length, horizontal the eigenvector number.

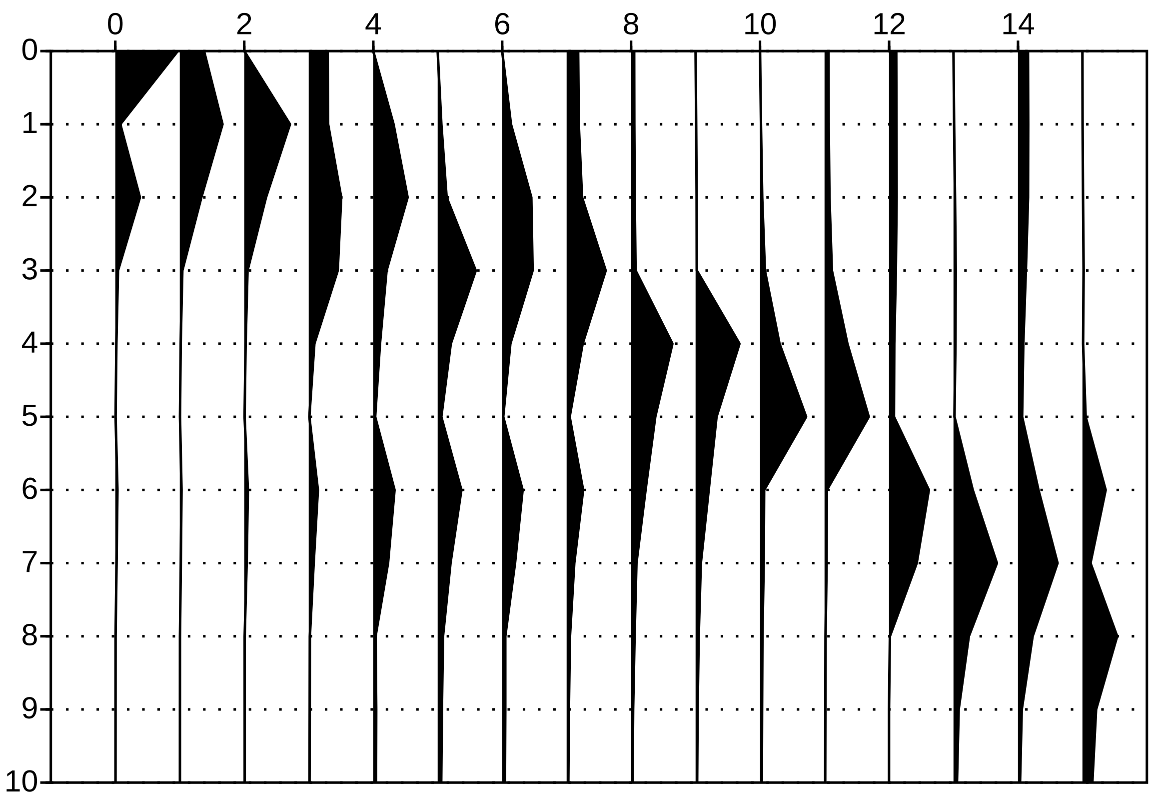

Figure 26: Amplitude of spectrum of eigenvalues of $\mathbf{T}^H\mathbf{T}$

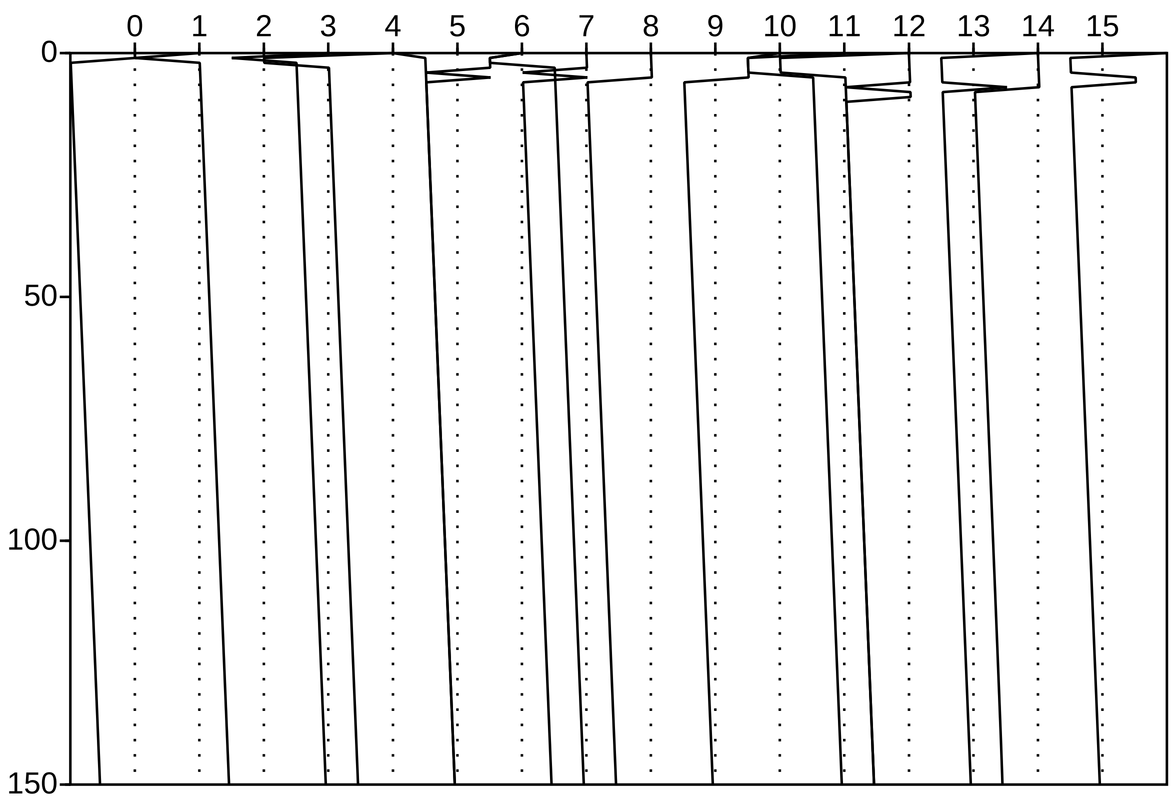

Figure 27: Phase of spectrum of eigenvalues of $\mathbf{T}^H\mathbf{T}$

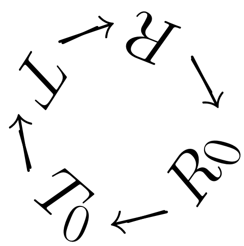
R
R_0
T_0
T

4.2 Influence of boundaries 1D medium

To check the influence of the boundaries of matrix $\mathbf{R}^H\mathbf{R}$ (or $\mathbf{T}^H\mathbf{T}$) on the eigenvalue decomposition, we consider a 1D medium with a high-contract layer between 100 and 300 m depth (3 layer medium 1000-4000-1000 m/s, the thickness of 200 m gives a $4000/400 = 0.1$ s. internal multiple train). The data has been modeled with a fixed spread acquisition geometry and a point source. With this velocity model $\mathbf{T}^H\mathbf{T}$ is a Hermitian Toeplitz matrix. For this 1D model the eigenvalue decomposition should give an exact decomposition in plane wave responses.

Figure 28 shows the calculated eigenvalues in $\tau - p$ domain, where different algorithms (assuming different boundaries) are used to calculate the eigenvalues. Using FFT's, which is equivalent to assuming a circular extension of the matrix, produces clean eigenvalues as shown in Figure 28a. By extending the Toeplitz matrix to a circular matrix (the matrix has then dimemsions which are 2 times larger (131 points)), and using a general eigenvalue solver from LAPACK, gives the same results as shown in Figure 28b. Using the Hermitian structure of the matrix, (by using a less general solver), and the circular extension gives the same results (Figure 28c). However, by returning to the original problem, and leaving out the circular extension, both the general solver (Figure 28d) and the Hermitian solver (Figure 28e) give less clean results. Applying a 15 point cosine taper to the edges of the 66x66 points matrix, does not improve the results of the eigenvalue decomposition (Figure 28f).

From these experiments we observe that the eigenvalue solvers (LAPACK's ZGEEV and ZHEEVX) give less clean results due to boundary effects. There migth also be an effect due to the inaccurate sorting of the eigenvalues, although it is expected to be small, since for a 1D medium the sorting is not that difficult. By using FFT's, or extending the matrix to become circular, gives clean results.

Note that the eigenvalue decomposition has been checked by reproducing the $\mathbf{R}^H\mathbf{R}$ using $\mathbf{R}^H\mathbf{R} = \mathbf{L}\mathbf{\Lambda}_r\mathbf{L}^H$.

4.3 Summary of the assumptions made in the derivation

O'Doherty and Anstey [] found that the coda operator $C(\omega)$ is related to the power spectrum of the reflection coefficient. (See discussion in proefschrift Frederic: pages 18-19-20 section 2.4.) For the current discussion we only need the know that C can be written as:

$$C(p, \mathbf{x}_A, \Delta z) = \exp(-\mathcal{A}(p)\Delta z) \tag{46}$$

This assumes a set of 1D (thin) layers. We need to resolve $\mathbf{C}$ from $\mathbf{C}^H\mathbf{C}$ and make the assumption that:

$$\mathbf{C} = \mathbf{L}\mathbf{\Lambda}_c\mathbf{L}^H \tag{47}$$

$$\mathbf{\Lambda}_c(p) = \exp\{-\underset{\sim}{\mathbf{A}}(p)(\omega)\Delta z_{tot}\} \tag{48}$$

$$\mathbf{\Lambda}_c(p) = \begin{pmatrix} e^{-\mathcal{A}(p_1)\Delta z_{tot}} & 0 & \dots & 0 \\ 0 & e^{-\mathcal{A}(p_2)\Delta z_{tot}} & \dots & 0 \\ \dots & \dots & \dots & \dots \\ 0 & 0 & \dots & e^{-\mathcal{A}(p_N)\Delta z_{tot}} \end{pmatrix} \tag{49}$$

where $\underset{\sim}{\mathbf{A}}(p)$ is a diagonal matrix. For plane waves in 1D media $\mathbf{C}$ is a circulant matrix which has the property that its Fourier transform is equal to its eigenvalues (see [Sjöström, 1996] for proof): $\mathbf{\Lambda}_c = \mathcal{F}_{x \to k_x}\{\mathbf{C}\}$ $\mathbf{C} = \mathbf{F}^H\mathbf{\Lambda}_c\mathbf{F}$

Correlation of coda matrix:

$$\mathbf{C}^H\mathbf{C} = \mathbf{L}\mathbf{\Lambda}_c^H\mathbf{\Lambda}_c\mathbf{L}^H \tag{50}$$

$$\mathbf{\Lambda}_c^H\mathbf{\Lambda}_c = \exp\{-2\Re\{\underset{\sim}{\mathbf{A}}(p)\}\Delta z_{tot}\} \tag{51}$$

$$\mathbf{\Lambda}_c^H\mathbf{\Lambda}_c = \begin{pmatrix} e^{-2\Re\{\mathcal{A}_1\}} & 0 & \dots & 0 \\ 0 & e^{-2\Re\{\mathcal{A}_2\}} & \dots & 0 \\ \dots & \dots & \dots & \dots \\ 0 & 0 & \dots & e^{-2\Re\{\mathcal{A}_N\}} \end{pmatrix} \tag{52}$$

Using the assumptions about the coda operator the $\underset{\sim}{\mathbf{A}}(p)$ operator can be retrieved from its real part. The main assumption states that the elements $A_l(\omega)$ of $\underset{\sim}{\mathbf{A}}(p)$ are the Fourier transforms of causal filters in the time domain. This is true for 1D media, since in that case $\underset{\sim}{\mathbf{A}}$ is the spatial fourier transform of $\underset{\sim}{\mathbf{C}}$, so $A_l(\omega) = \tilde{\mathcal{A}}_l(k_{x,l}, \omega)$. Note that before the temporal Fourier transforms yields the causal filters, the diagonal elements must to be scaled from wavenumber k_x to propagation angle p with $\frac{1}{\omega}(k_x = p\omega)$. Also in the general 3-D case a scaling of the diagonal of $\underset{\sim}{\mathbf{\Lambda}}_c$ with $\frac{1}{\omega}$ is reguired before the $A_l(\omega)$ can be interpreted as the Fourier transforms of causal filters in the time domain.

Using mutations of the $\mathbf{T}^H\mathbf{T}$ matrix we have tried to make the matrix more circular. The calculated eigenvalues still show a noisy appearance.

Test on pseudo 1D model, Reconstruct Coda from calculated eigenvalues.

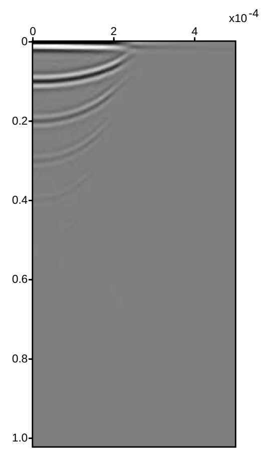

a) FFT

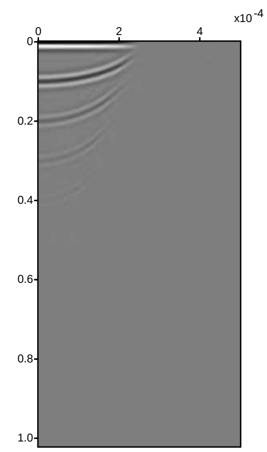

b) Circular with general Lapack (ZGEEV)

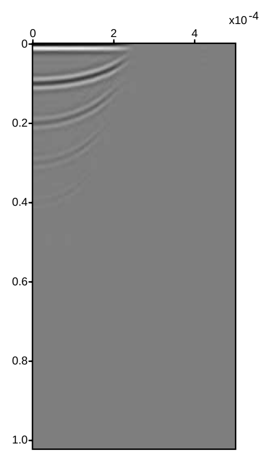

c) Circular with Hermitian Lapack (ZHEEVX)

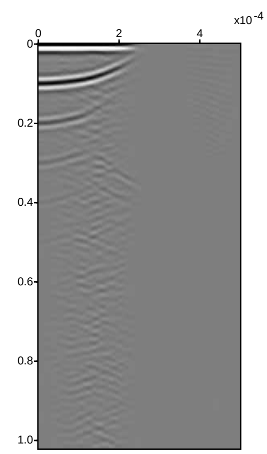

d) General Lapack (ZGEEV)

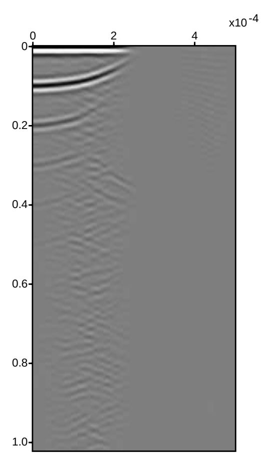

e) Hermitian Lapack (ZHEEVX)

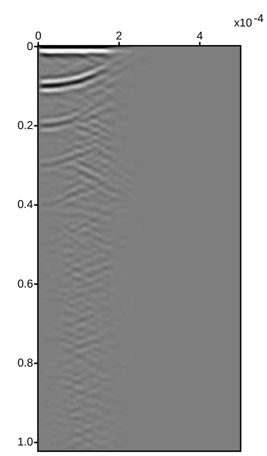

f) Hermitian Lapack (ZHEEVX) and 15 point taper

Figure 28: Eigenvalues in $\tau - p$ with different treatment of the boundaries and using different eigenvalue decompositions of the $\mathbf{T}^H\mathbf{T}$ matrix.

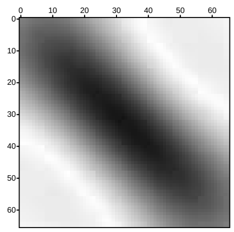

a) matrix for 2 Hz

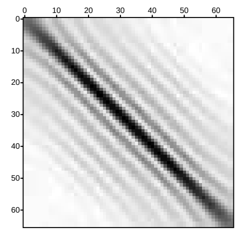

b) matrix for 25 Hz

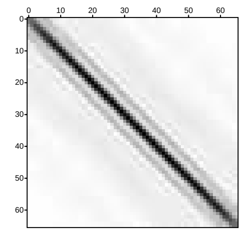

c) matrix for 50 hz

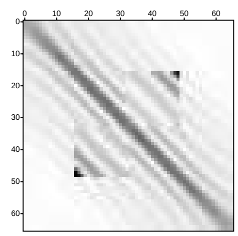

d) full ’folded’ matrix for 25 hz

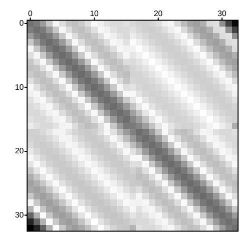

e) folded matrix for 25 hz

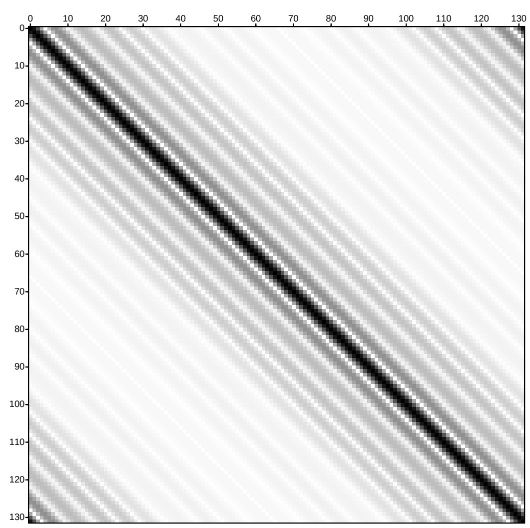

e) circulant matrix of 25 Hz

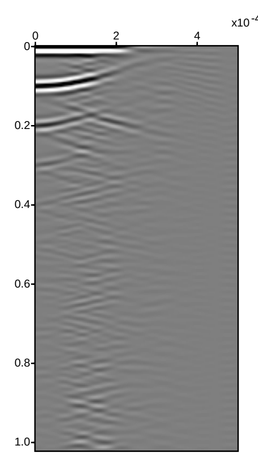

f) eigenvalues for folded matrix e

Figure 29: frequency slices of the $\mathbf{T}^H\mathbf{T}$ matrix and mutations of that matrix.

4.4 2D medium simple media

4.5 2D medium complex media

To calculate the eigenvalues of $\mathbf{R}^H\mathbf{R}$ for the medium shown in Figure 31, we must use a general (ZGEEV) or Hermitain (ZHEEV) eigenvalue solver to be able to handle the complexity of the $\mathbf{T}^H\mathbf{T}$ matrix. These solvers gives very noisy results, shown in Figure 31a and b, due to boundary effects, inaccurate sorting of the eigenvalues, and the 1D assumption included in the method itself. Extending the complete matrix to a circular form is not possible.

However, it is possible to use FFT's on one of the columns of the matrix and assuming that this selected column is embedded in a 1D medium. This gives the results as shown in Figure 31c,d,e and f for different columns. At this moment it is unclear if these estimated operators can still be used? Note that for columns other than the first, the transformation to ray-parameter p should to be adjusted to a new reference frame. This is not yet done in Figure 31d,e and f.

The cross-correlation matrix is written as:

$$R_c(\mathbf{x}_A, \mathbf{x}_B) = \int_{\partial\mathcal{D}_0} R_0^*(\mathbf{x}, \mathbf{x}_A) R_0(\mathbf{x}, \mathbf{x}_B) d^2\mathbf{x}_H \tag{53}$$

One column of the cross-correlation matrix R_c at position $\mathbf{x}_{A_1}$ represents the cross correlation between all shot records with the shot record at $\mathbf{x}_{A_1}$, followed by a summation over the receiver positions. Assuming a local 1D medium the eigenvalues of this column can be calculated using FFT's. This can be done for all columns ($\mathbf{x}_{A_1}$ positions) in the matrix.

The eigenvalue decomposition with 1D assumption for every row in $\mathbf{R}^H\mathbf{R}$ and selection of the horizontal plane wave ($p = k_x = 0$) can be written as

$$\tilde{R}_c(k_{x,A}, \mathbf{x}_B) = \int R_c(\mathbf{x}_A, \mathbf{x}_B) \exp\left(-jk_{x,A}x_A\right) d\mathbf{x}_A \tag{54}$$

$$\tilde{R}_c(0, \mathbf{x}_B) = \int R_c(\mathbf{x}_A, \mathbf{x}_B) d\mathbf{x}_A \tag{55}$$

By selecting other, non-horizontal, ray-parameters it is possible to construct 1D solutions for all 'positions'(columns) in the model using a 1D assumption at every 'position' in the matrix. This is shown in Figure 32 for different ray-parameters.

4.5.1 Usage of the estimated coda operators

$$\delta(\mathbf{x}_{H,A} - \mathbf{x}_{H,B}) - \int_{\partial\mathcal{D}_0} R_0^*(\mathbf{x}, \mathbf{x}_A) R_0(\mathbf{x}, \mathbf{x}_B) d^2\mathbf{x}_H = \int_{\partial\mathcal{D}_m} T_0^*(\mathbf{x}, \mathbf{x}_A) T_0(\mathbf{x}, \mathbf{x}_B) d^2\mathbf{x}_H \tag{56}$$

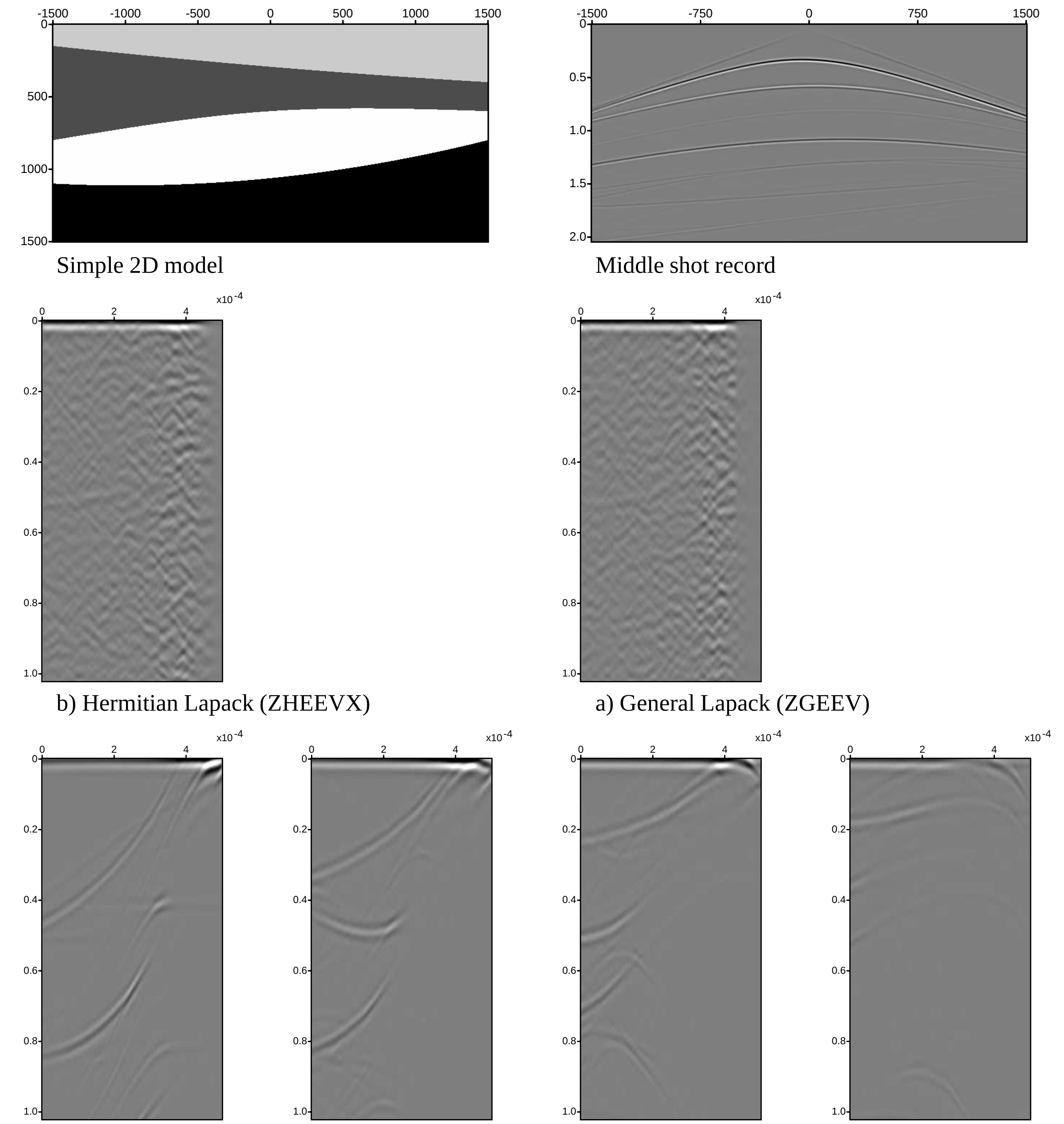

Simple 2D model

Middle shot record

b) Hermitian Lapack (ZHEEVX)

a) General Lapack (ZGEEV)

c) FFT of 1 column

d) FFT of 76 column

e) FFT of 151 column

f) FFT of 226 column

Figure 30: Eigenvalues in $\tau - p$ for a simple 2D medium.

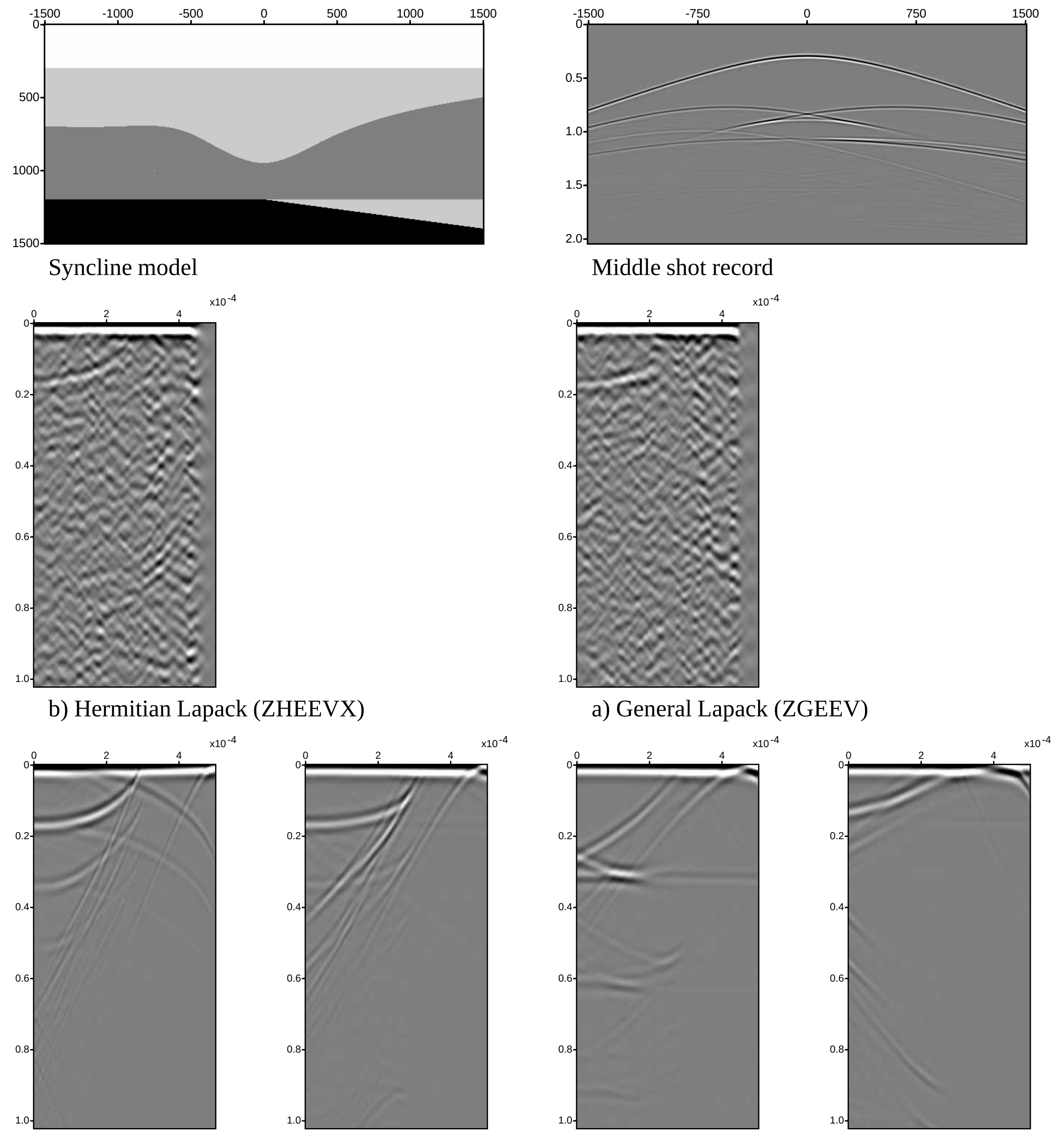

Syncline model

Middle shot record

b) Hermitian Lapack (ZHEEVX)

a) General Lapack (ZGEEV)

c) FFT of 1 column

d) FFT of 50 column

e) FFT of 101 column

f) FFT of 150 column

Figure 31: Eigenvalues in $\tau - p$ for a simple 2D medium.

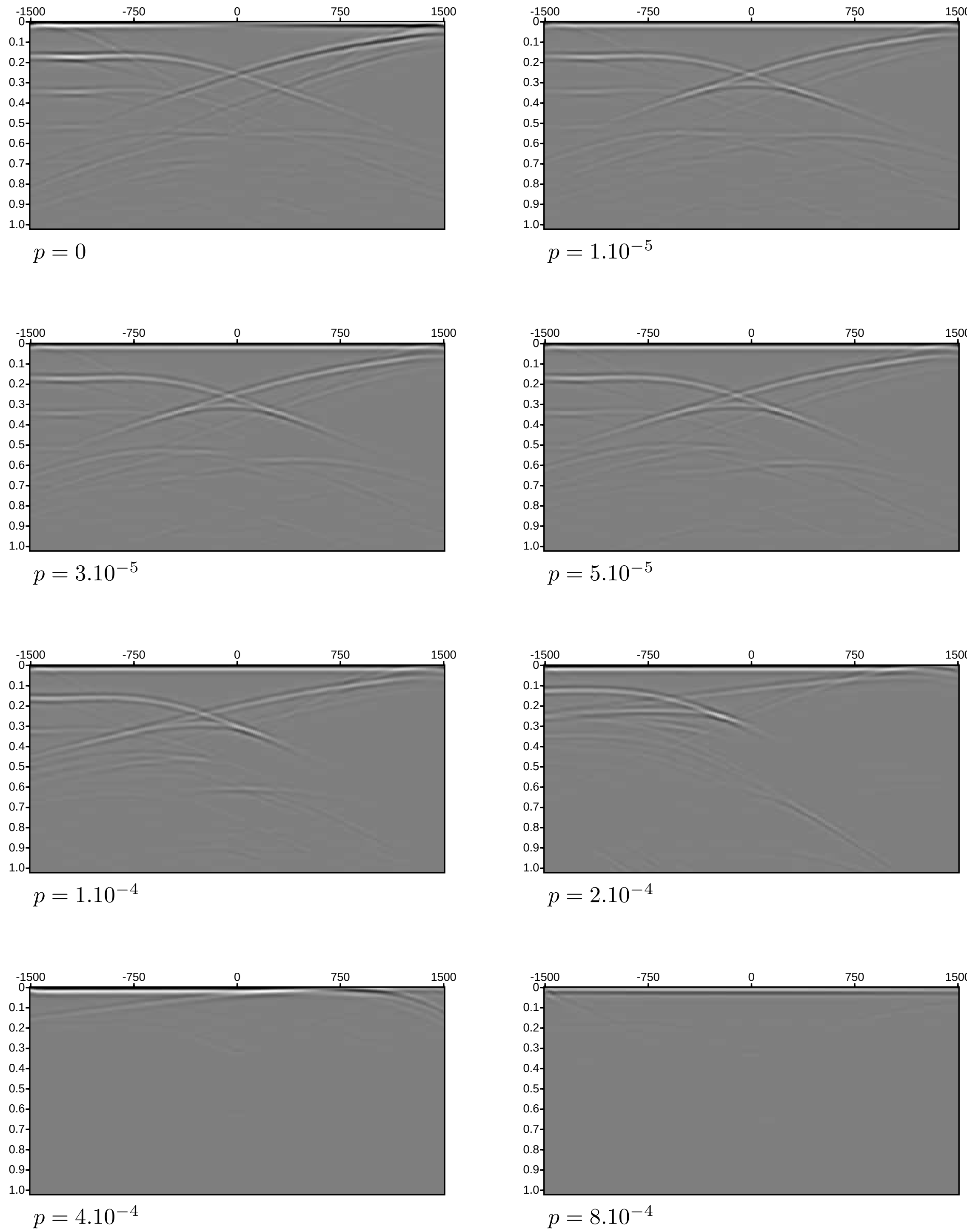

Figure 32: Calculated eigenvalues for different p values assuming local plane waves.

4.6 2D realistic media

4.6.1 Marmousi

4.6.2 SEG/EAGE salt-dome model

From reflection to transmission and back to reflection.

examples on measured data, triax-bank, waterbak.

5 Extension to 3D

References

[Bar-On and Ryaboy, 1997] Bar-On, I. and Ryaboy, V. (1997). Fast diagonalization of large and dense complex symmetric matrices, with applications to quantum reaction dynamics. *SIAM Journal on Scientific Computing*, 18(5):1412–1435.

[Bracewell, 1986] Bracewell, R. N. (1986). *The Fourier transform and its applications, second edition*. McGraw-Hill, Singapore.

[Sjöström, 1996] Sjöström, E. (1996). *Singular Value Computations for Toeplitz Matrices*. PhD thesis, Department of Mathematics, Linköping University Sweden.